https://doi.org/10.5194/essd-2021-53
Preprint. Discussion started: 24 March 2021

Open Access Earth System Science Data Discussions

A 1-km global dataset of historical (1979-2017) and future (2020-2100) Köppen-Geiger climate classification and bioclimatic variables

Diyang Cui[1], Shunlin Liang[1], Dongdong Wang[1], Zheng Liu[1]

[1]Department of Geographical Sciences, University of Maryland, College Park, 20740, USA

Correspondence to: Shunlin Liang(sliang@umd.edu)

Abstract.

The Köppen-Geiger climate classification scheme provides an effective and ecologically meaningful way to characterize climatic conditions and has been widely applied in climate change studies. The Köppen-Geiger climate maps currently available are limited by relatively low spatial resolution, poor accuracy, and noncomparable time periods. Comprehensive assessment of climate change impacts requires a more accurate depiction of fine-grained climatic conditions and continuous long-term time coverage. Here, we present a series of improved 1-km Köppen-Geiger climate classification maps for ten historical periods in 1979-2017 and four future periods in 2020-2099 under RCP2.6, 4.5, 6.0, and 8.5. The historical maps are derived from multiple downscaled observational datasets and the future maps are derived from an ensemble of bias-corrected downscaled CMIP5 projections. In addition to climate classification maps, we calculate 12 bioclimatic variables at 1-km resolution, providing detailed descriptions of annual averages, seasonality, and stressful conditions of climates. The new maps offer higher classification accuracy and demonstrate the ability to capture recent and future projected changes in spatial distributions of climate zones. On regional and continental scales, the new maps show accurate depictions of topographic features and correspond closely with vegetation distributions. We also provide a heuristic application example to detect long-term global-scale area changes of climate zones. This high-resolution dataset of Köppen-Geiger climate classification and bioclimatic variables can be used in conjunction with species distribution models to promote biodiversity conservation and to analyse and identify recent and future interannual or interdecadal changes in climate zones on a global or regional scale. The dataset referred to as KGClim, is publicly available at http://doi.org/10.5281/zenodo.4546140 for historical climate and http://doi.org/10.5281/zenodo.4542076 for future climate.

1 Introduction

Climate is a key driver of ecosystem functioning and processes, and has a direct impact on the distribution of species (Chen, Hill, Ohlemüller, Roy, & Thomas, 2011; Ordonez & Williams, 2013; Pinsky, Worm, Fogarty, Sarmiento, & Levin, 2013; Thuiller, Lavorel, Araújo, Sykes, & Prentice, 2005). The spatial patterns of climates have been often identified using the Köppen climate classification system (Köppen, 1931).

https://doi.org/10.5194/essd-2021-53
Preprint. Discussion started: 24 March 2021

The Köppen classification system is based on annual cycles of surface air temperature and precipitation. It was designed to empirically map the distributions of the world's biomes (Köppen, 1936). Compared with other human expertise based climate mapping methods (e.g., Holdridge, 1947; Thornthwaite, 1931; Walter & Elwood, 1975) and clustering approaches (e.g., Netzel & Stepinski, 2016), which suffer from a lack in meteorological basis, the Köppen classification demonstrates stronger correlation with distributions of biomes and soil types (Bockheim, Gennadiyev, Hammer, & Tandarich, 2005; Rohli, Joyner, Reynolds, & Ballinger, 2015). It provides an ecologically relevant and effective method to characterize climate conditions by incorporating the seasonal cycles of surface air temperature and precipitation.

As a convenient and integrated tool to identify spatial patterns of climatic variables and to examine relationships between climates and biological systems, the Köppen classification has been widely applied in biological science, earth and planetary sciences, and environmental science (Rubel & Kottek, 2011). It has been found useful for a variety of issues on climate change, such as hydrological cycle studies (Manabe & Holloway, 1975; Peel, McMahon, Finlayson, & Watson, 2001), Arctic climate change (Feng et al., 2012; Wang & Overland, 2004), assessment of climate change impacts on ecosystem (Roderfeld et al., 2008), biome distribution (Leemans, Cramer, & van Minnen, 1996; Rohli, Joyner et al., 2015) and biodiversity (Garcia, Cabeza, Rahbek, & Araújo, 2014).

There has been a resurgence in popularity of the Köppen climate classification (Cui, Liang, & Wang, 2021). The Köppen climate classification has been often used to set up dynamic global vegetation models (Poulter et al., 2011), to model the species range distribution (Brugger & Rubel, 2013; Tererai & Wood, 2014; Webber et al., 2011), and to analyze the species growth behavior (Tarkan & Vilizzi, 2015). The Köppen classification has also been applied to detect the shifts in geographical distributions of climate zones (Belda, Holtanová, Kalvová, & Halenka, 2016; Chan & Wu, 2015; Feng et al., 2014; Mahlstein, Daniel, & Solomon, 2013). The Köppen climate classification demonstrates the ability to aggregate complex and diverse climate gradients into ecologically meaningful classes and simplify spatial variability. It gives a new direction to develop climate change metrics and provides support for the growth of species distribution modelling (SDM), in the fields of biogeography, ecology and biodiversity conservation.

The availability of gridded datasets of climatic variables with global coverage enabled creation of global maps of Köppen climates (Cui, Liang, & Wang, 2021). Most current Köppen climate classification maps are limited by a relatively low resolution of 0.5° (Belda, Holtanová, Halenka, & Kalvová, 2014; Grieser, Gommes, Cofield, & Bernardi, 2006; Kottek, Grieser, Beck, Rudolf, & Rubel, 2006; Kriticos et al., 2012; Rubel & Kottek, 2010). Several map products used interpolation methods to obtain a higher resolution of ~0.1° (Kriticos et al., 2012; Peel, Finlayson, & McMahon, 2007; Rubel, Brugger, Haslinger, & Auer, 2017). However, fine resolutions of at least 1-km are required to detect relevant microrefugia and promote effective conservation. In addition, climate maps, which were derived using a limited number of data sources, were based on a considerably small number of ground stations with highly uneven distributions. This eventually led to widespread misclassifications of Köppen climates, particularly in mountainous regions with strong climatic gradients and often low station density (Karger et al., 2017).

https://doi.org/10.5194/essd-2021-53
Preprint. Discussion started: 24 March 2021

Focus should be put onto the improvement of data integration of the current observational climatology data and future model projections to increase both the accuracy and resolution (Cui, Liang, & Wang, 2021). Beck et al. (2018) presented new global climate classification maps with 1-km resolution for two periods of 1980–2016 and 2071–2100. However, its single and non-comparable period coverage cannot sufficiently fulfil the needs of climate change research. Significant changes in Köppen climates have been observed and projected in recent centuries (Belda et al., 2014; Chan & Wu, 2015; Chen & Chen, 2013; Rohli, Andrew, Reynolds, Shaw, & Vázquez, 2015; Yoo & Rohli, 2016). Previous studies found that large-scale shifts in climate zones have been observed over more than 5% of the total land area since the 1980s (Cui, Liang, & Wang, 2021). Detection of interannual or interdecadal climate changes with the application of Köppen climate maps needs more accurate depiction of fine-grained climatic conditions, and continuous long-term temporal coverage.

Therefore, there is a strong need to compile a series of global maps of Köppen climate classification with finer spatial and temporal resolutions, and improved accuracy. Multiple global observational datasets of temperature and precipitation collected during the recent centuries, and global climate simulations have offered the possibility to create a comprehensive dataset for past and future climates. In this study, we presented an improved long-term climate classification map series for 1) ten historical 30-yr periods of the observational record (1979-2008,1980-2009…1988-2017) and four future 30-yr periods (2020-2049, 2040-2069, 2060-2089, 2070-2099) under four RCPs (RCP2.6, 4.5, 6.0 and 8.5). To improve the classification accuracy and achieve a resolution as fine as 1-km (30 arc-second), we combined multiple datasets, including WorldClim V2 (Fick & Hijmans, 2017), CHELSA V1.2 (Karger et al., 2017), CRU TS v4.03 (New, Hulme, & Jones, 2000), UDEL (Willmott & Matsuura, 2001), GPCC datasets (Beck, Grieser, & Rudolf, 2005) and bias-corrected downscaled Coupled Model Intercomparison Project Phase 5 (CMIP5) model simulations (Navarro-Racines, Tarapues, Thornton, Jarvis, & Ramirez-Villegas, 2020) (Table 1). We also calculated 12 bioclimatic variables at the same 1-km resolution using these climate datasets for the same historical and future periods. This dataset can be used to in conjunction with SDMs to promote biodiversity conservation, or to analyse and identify recent and future changes in climate zones on a global or regional scale.

To validate the Köppen-Geiger climate classification maps, we used the station observations from Global Historical Climatology Network-Daily (GHCN-D) (Menne, Durre, Vose, Gleason, & Houston, 2012), and Global Summary Of the Day (GSOD) (National Climatic Data Center, NESDIS, NOAA, & U.S. Department of Commerce, 2015) database. At the regional and continental scale, we compared our Köppen-Geiger climate classification maps with previous map products, associated maps of forest cover, and elevation distribution, for 1) regions with large spatial gradients in climates, including central and eastern Africa, Europe, North America, and 2) regions with sharp elevation gradients, including Tibetan Plateau, central Rocky Mountains, central Andes. Further, we conducted sensitivity analysis with respect to classification temporal scale, dataset input, and data integration methods. We also provided a heuristic example which used climate classification map series to detect the long-term area changes of climate zones, showing how the Köppen-Geiger climate classification map series can be applied in climate change studies.

https://doi.org/10.5194/essd-2021-53
Preprint. Discussion started: 24 March 2021

Open Access Earth System Science Data Discussions

2 Datasets

Table 1 Climatology datasets to generate present global maps of Köppen climate classification with varied spatial resolutions

Dataset	Spatial Resolution	Temporal Span	Variable(s)	Source and Description
Present Köppen classification map series with resolution of 30 arc-second (1km)				
CRU	0.5°	1979-2017	T	Climatic Research Unit (CRU) TS v4.03
UDEL	0.5°	1979-2017	T, P	U. of Delaware Precipitation and Air Temperature
WorldClim	0.0083°	1970-2000	T, P	WorldClim Historical Climate Data V2
CHELSA	0.0083°	1979-2013	T, P	Climatologies at high resolution for the earth's land surface areas (CHELSA)
GPCC	0.5°	1979-2016	P	Global Precipitation Climatology Centre (GPCC)
Future Köppen classification map series with resolution of 30 arc-second (1km)				
CMIP5	0.0083°	2020-2100	T, P	CCAFS-Climate Statistically Downscaled Delta Method CMIP5 data
WorldClim	0.0083°	1970-2000	T, P	WorldClim Historical Climate Data V2

Table 1 lists the climatology datasets with global coverage and on a monthly time step, used to generate historical and future Köppen-Geiger climate map series. The present 1-km Köppen-Geiger classification map series for 1979-2017 was derived from the Climatologies at High-resolution for the Earth's Land Surface Areas (CHELSA) V1.2 (Karger et al., 2017), WorldClim Historical Climate Data V2 (Fick & Hijmans, 2017) and the statistically downscaled Climatic Research Unit (CRU) TS v4.03 (New et al., 2000), University of Delaware Precipitation and Air Temperature (UDEL) (Willmott & Matsuura, 2001) and Global Precipitation Climatology Centre (GPCC) (Beck et al., 2005) datasets. To decide the datasets to use, we conducted a sensitivity analysis on the input climatology datasets and utilized monthly air temperature datasets from CRU, UDEL, GHCN_CAMS Gridded 2m Temperature (Fan & Dool, 2008) and monthly precipitation datasets from GPCC, UDEL, NOAA's PRECipitation REConstruction over Land (PREC/L) (Chen, Xie, Janowiak, & Arkin, 2002). Evaluation results indicated that incorporating only CRU, UDEL temperature datasets and UDEL, GPCC precipitation datasets led to higher accuracy in the classification results. Therefore, we chose CRU, UDEL, and GPCC datasets as the classification system input to boost the final accuracy.

To explicitly correct topographic effect, we used 1-km CHELSA V1.2 and WorldClim V2 datasets in addition to the 0.5° resolution datasets. The CHELSA dataset downscaled the model output temperature and precipitation of the ERA-Interim climatic reanalysis. Temperatures are derived using statistical downscaling method. Precipitations are based on algorithm incorporating many orographic predictors, including valley exposition, wind fields, and boundary layer height, and are bias corrected subsequently (Karger et al., 2017). With major topo-climatic drivers considered, the CHELSA dataset demonstrated good performance in ecological science studies. Validated with the station data from Global Historical Climate Network (Menne et al., 2012) and other products, CHELSA data exhibited comparable accuracy for temperatures and better predicted precipitation patterns.

https://doi.org/10.5194/essd-2021-53
Preprint. Discussion started: 24 March 2021

Open Access Earth System Science Data Discussions

Table 2 CMIP5 GCMs for four Representative Concentration Pathways (RCPs), used to generate future Köppen climate map series.

Model	Institute	RCP2.6	RCP4.5	RCP6.0	RCP8.5
BCC-CSM1.1	Beijing Climate Center, China Meteorological Administration	√	√	√	√
BCC-CSM1.1(m)	Beijing Climate Center, China Meteorological Administration	√	√	√	√
BNU-ESM	Beijing Normal University	√	√		√
CCCMA-CanESM2	Canadian Centre for Climate Modelling and Analysis	√	√		√
CESM1-BGC	National Science Foundation, Department of Energy, National Center for Atmospheric Research		√		√
CESM1-CAM5	National Science Foundation, Department of Energy, National Center for Atmospheric Research	√	√	√	√
CNRM-CM5	Centre National de Recherches Meteorologiques and Centre Europeen de Recherche et Formation Avancees en Calcul Scientifique	√	√		√
CSIRO-ACCESS1.0	Commonwealth Scientific and Industrial Research Organization (CSIRO) and Bureau of Meteorology (BOM), Australia		√		√
CSIRO-ACCESS1.3	Commonwealth Scientific and Industrial Research Organization (CSIRO) and Bureau of Meteorology (BOM), Australia		√		√
CSIRO-Mk3.6.0	Queensland Climate Change Centre of Excellence and Commonwealth Scientific and Industrial Research Organization	√	√	√	√
EC-EARTH	European Centre for Medium-Range Weather Forecasts (ECMWF)				√
FIO-ESM	The First Institute of Oceanography, State Oceanic Administration, China	√	√	√	√
GFDL-CM3	NOAA Geophysical Fluid Dynamics Laboratory	√	√	√	√
GFDL-ESM2G	NOAA Geophysical Fluid Dynamics Laboratory	√	√	√	√
GFDL-ESM2M	NOAA Geophysical Fluid Dynamics Laboratory	√	√	√	√
GISS-E2H	NASA Goddard Institute for Space Studies USA	√		√	√
GISS-E2HCC	NASA Goddard Institute for Space Studies USA		√		
GISS-E2R	NASA Goddard Institute for Space Studies USA	√	√	√	√
GISS-E2RCC	NASA Goddard Institute for Space Studies USA		√		
INM-CM4	Institute of Numerical Mathematics of the Russian Academy of Sciences		√		√
IPSL-CM5A-LR	Institut Pierre Simon Laplace	√	√	√	√
IPSL-CM5A-MR	Institut Pierre Simon Laplace	√	√		√
IPSL-CM5B-LR	Institut Pierre Simon Laplace				√
LASG-FGOALS-G2	Institute of Atmospheric Physics (LASG) and Tsinghua University (CESS)	√	√		
MIROC-ESM	University of Tokyo, National Institute for Environmental Studies and Japan Agency for Marine-Earth Science and Technology	√	√	√	
MIROC-ESM-CHEM	University of Tokyo, National Institute for Environmental Studies and Japan Agency for Marine-Earth Science and Technology	√	√	√	

https://doi.org/10.5194/essd-2021-53
Preprint. Discussion started: 24 March 2021

Open Access Earth System Science Data Discussions

MIROC-MIROC5	University of Tokyo, National Institute for Environmental Studies and Japan Agency for Marine-Earth Science and Technology	√	√	√	√
MOHC-HadGEM2-CC	UK Met Office Hadley Centre		√		√
MOHC-HadGEM2-ES	UK Met Office Hadley Centre	√	√	√	√
MPI-ESM-LR	Max Planck Institute for Meteorology	√	√		√
MPI-ESM-MR	Max Planck Institute for Meteorology	√			√
MRI-CGCM3	Meteorological Research Institute	√	√	√	√
NCAR-CCSM4	US National Centre for Atmospheric Research	√	√	√	√
NCC-NorESM1-M	Norwegian Climate Centre	√	√	√	√
NIMR-HadGEM2-AO	National Institute of Meteorological Research and Korea Meteorological Administration	√	√	√	√

We produced the future Köppen classification map series using the CCAFS climate statistically bias-corrected and downscaled CMIP5 projections (Navarro-Racines et al., 2020). The CCAFS presented a global database of future climates developed by a climate model bias correction method based on the CMIP5 GCM simulations (Taylor, Stouffer, & Meehl, 2012) archive, coordinated by the World Climate Research Programme in support of the IPCC Fifth Assessment Report (AR5) (Hartmann et al., 2013). The total is 35 GCMs, and all RCPs, RCP 2.6, 4.5, 6.0 and 8.5 (Table 2). Projections are available at varied coarse scales (70–400km). To achieve high-resolution (1km) climate representations, downscaling method has been applied with the use of the WorldClim data (Fick & Hijmans, 2017). Technical evaluatwq8iion showed that the bias-correction method that CCAFS data applied reduced climate model bias by 50–70%, which could potentially address the bias issue in model simulations for the threshold-based Köppen classification scheme.

3 Methodology

3.1 Köppen-Geiger climate classification

Table 3 Criteria of Köppen-Geiger climate classification with temperature in oC and precipitation in mm.

1st	2nd	3rd	Description	Criterion
A			Tropical	Not (B) & T_{cold}≥18
	f		- Rainforest	P_{dry}≥60
	m		- Monsoon	Not (Af) & P_{dry}≥100-*MAP*/25
	w		- Savannah	Not (Af) & P_{dry}<100-*MAP*/25
B			Arid	*MAP*<10×$P_{threshold}$
	W		- Desert	*MAP*<5×$P_{threshold}$
	S		- Steppe	*MAP*≥5×$P_{threshold}$
		h	-- Hot	*MAT*≥18

https://doi.org/10.5194/essd-2021-53
Preprint. Discussion started: 24 March 2021

Open Access Earth System Science Data Discussions

		k	-- Cold	MAT<18
C			Temperate	Not (B) & T_{hot}>10 & -3 <T_{cold}<18
	w		- Dry winter	P_{wdry}<P_{swet}/10
	s		- Dry summer	*Not (w)* & P_{sdry}<40 & P_{sdry}<P_{wwet}/3
	f		- Without dry season	Not (s) or (w)
		a	-- Hot summer	T_{hot}≥22
		b	-- Warm summer	Not (a) & T_{mon10}≥4
		c	-- Cold summer	Not (a or b) & 1≤T_{mon10}<4
D			Boreal	Not (B) & T_{hot}>10 & T_{cold}≤-3
	w		- Dry winter	P_{wdry}<P_{swet}/10
	s		- Dry summer	*Not (w)* & P_{sdry}<40 & P_{sdry}<P_{wwet}/3
	f		- Without dry season	Not (s) or (w)
		a	- Hot summer	T_{hot}≥22
		b	- Warm summer	Not (a) & T_{mon10}≥4
		c	- Cold summer	Not (a), (b) or (d)
		d	- Very cold winter	Not (a) or (b) & T_{cold}<-38
E			Polar	Not (B) & T_{hot}≤10
	T		- Tundra	T_{hot}>0
	F		- Frost	T_{hot}≤0

MAT = mean annual air temperature (°C); T_{cold} = the air temperature of the coldest month (°C); T_{hot} = the air temperature of the warmest month (°C); T_{mon10} = the number of months with air temperature >10 °C; MAP = mean annual precipitation (mm y^{-1}); P_{dry} = precipitation in the driest month (mm $month^{-1}$); P_{sdry} = precipitation in the driest month in summer (mm $month^{-1}$); P_{wdry} = precipitation in the driest month in winter (mm $month^{-1}$); P_{swet} = precipitation in the wettest month in summer (mm $month^{-1}$); P_{wwet} = precipitation in the wettest month in winter (mm $month^{-1}$); $P_{threshold}$=2×MAT if >70% of precipitation falls in winter, $P_{threshold}$=2×MAT+28 if >70% of precipitation falls in summer, otherwise $P_{threshold}$=2×MAT+14.

As the first quantitative classification system of Earth's climates, the Köppen climate classification was introduced by Wladimir Köppen in 1900. Its modification, Köppen-Geiger classification (KGC) (Köppen, 1884; Köppen, 1936) is the most frequently used system. First published in 1936 (Köppen, 1936), developed by Wladimir Köppen and Rudolf Geiger, KGC identifies climates based on their effects on plant growth from the aspects of warmth and aridity, and classifies climate into five main climate classes and 30 subtypes (Rubel & Kottek, 2011). The five main vegetation groups distinguish between plants of the tropical zone (A), the arid zone (B), the temperate zone (C), the snow zone (D) and the polar zone (E), referring to the five major climate zones (Sanderson, 1999). Only arid (B) climate zone is defined based on precipitation threshold and the others are thermal zones.

This research followed the Köppen-Geiger climate classification as described in Kottek et al. (2006), and Rubel and Kottek (2010). This latest version of the KGC scheme was first presented by Geiger (1961) (Table 3) while existing Köppen-Geiger climate map products, including Peel et al. (2007), Kriticos et al. (2012) and Beck et al. (2018) applied the KGC scheme modified following Russell (1931). Russell (1931) adjusted the definition of the boundary of temperate (C) and boreal (D)

https://doi.org/10.5194/essd-2021-53
Preprint. Discussion started: 24 March 2021

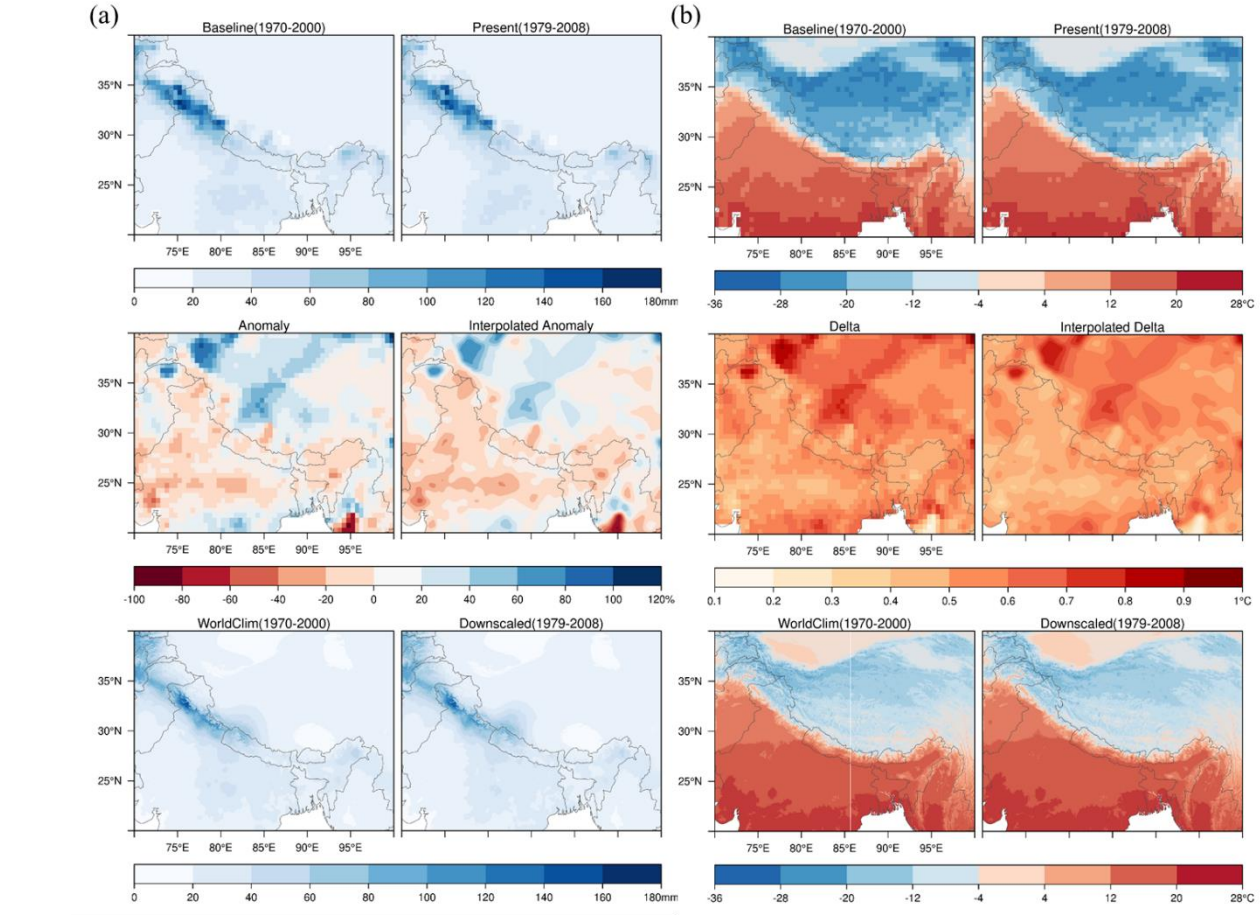

Figure 1. Illustration of the downscaling process. (a) Anomaly downscaling method with January total precipitation from GPCC dataset and (b) delta downscaling method with January temperature from CRU dataset. Baseline (1970-2000) and present-day climate data (e.g. 1979-2008) are from CRU, UDEL, or GPCC datasets, which have a coarse spatial resolution of 0.5°. Precipitation anomaly is change factor of monthly precipitation from baseline to present-day climates. Temperature delta is change in monthly air temperature from baseline to present-day climates. WorldClim (1970-2000) climate data is adjusted by multiplying 30 arc-second interpolated anomaly (for precipitation) or adding 30 arc-second interpolated delta (for temperature) to generate the downscaled climate surfaces with 30 arc-second resolution. Precipitation values in mm/month and temperature values in °C.

climate zones using the temperature of the coldest month > 0 °C instead of >-3 °C. The threshold was proposed because the 0°C line fits the distribution of the topographical features and vegetation in western United States, where at that time meteorological stations were sparsely distributed (Jones, 1932). However, the application of 0°C boundary to the global climates hasn't been validated. Therefore, this research didn't utilize the Russell's modification (1931) and followed the latest version KGC proposed by Geiger (1961).

3.2 Statistical downscaling

Due to limited number of available observational datasets with high resolution and long-term continuous temporal coverage, the research implemented the delta method by applying a delta change or change factor onto the WorldClim historical

https://doi.org/10.5194/essd-2021-53
Preprint. Discussion started: 24 March 2021


Open Access Earth System Science Data Discussions

observations (Fick & Hijmans, 2017) to achieve 30-yr average climatology data with a 1-km resolution based on the CRU, UDEL and GPCC datasets. The delta method is a statistical downscaling method that assumes that the relationship between climatic variables remain relatively constant at local scale. We applied delta method to downscale the long-term (30-yr) mean climates using coarse-resolution monthly climatology datasets. The delta change or change factor is calculated as the difference between the long-term (30-yr) means of temperature or precipitation of baseline (1970-2000) and present-day climates. The delta method comprises the following four steps: 1) calculate 30-yr averages for baseline (1970-2000) and present day of monthly temperature and precipitation; 2) calculate anomaly for precipitation and delta for temperature; 3) apply thin-plate splines interpolation (TPS) to derive 1km precipitation anomaly and temperature delta; 4) multiply anomaly or add delta to historical climates from WorldClim dataset (Fig. 1).

First, using monthly time series from CRU, UDEL and GPCC datasets, we calculated 30-yr means as a baseline (1970-2000), for each climatology dataset and each variable. We used 1970-2000 as baseline period, for consistency with WorldClim Historical Climate Data V2. Next, we calculated 30-yr means for each month and each 30-yr present-day period in 1979-2017. We then calculated anomalies as proportional differences between present-day and baseline in total precipitation and delta as difference in temperature. To derive 30 arc-second (1-km) anomaly or delta surfaces, we applied thin-plate splines (TPS) interpolation (Craven & Wahba, 1978; Franke, 1982; Schempp, Zeller, & Duchon, 1977) on precipitation anomaly and temperature delta. TPS has been widely used in climate science (Hijmans, Cameron, Parra, Jones, & Jarvis, 2005; Navarro-Racines et al., 2020) as it produced a smooth and continuous surface, which is infinitely differentiable. Last, we multiplied the change factor or added the delta to the WorldClim (1970-2000) data to get downscaled present-day monthly climate data.

The future Köppen-Geiger map series are based on an ensemble of maps from the CCAFS bias-corrected and downscaled climate projections from the 35 CMIP5 GCMs, and 4 RCPs (Navarro-Racines et al., 2020). Previous assessment studies showed that large areas, ranging from 20-50% of the total land area, have been misclassified by the GCMs with the reference climate maps established by observational data (Cui, Liang, & Wang, 2021). It is suggested that the uncertainties more likely to be attributable to deficiencies in model physics than grid size or limitations of the reference datasets (Tapiador, Moreno, & Navarro, 2019). To ensure better simulation results of climate classification, the multi-model ensemble mean or other pre-processing methods, such as the delta-change method (Hanf, Körper, Spangehl, & Cubasch, 2012), have been utilized to cope with the bias effects on the threshold-based classification scheme. Therefore, we utilized the CCAFS bias-corrected and downscaled CMIP5 projections (Navarro-Racines et al., 2020) to reduce the amplified errors due to uncertainty in climate projections. Navarro-Racines et al. (2020) applied delta method based on thin plate spline spatial interpolation of anomalies of original GCM outputs (Hay, Wilby, & Leavesley, 2000; Ho, Stephenson, Collins, Ferro, & Brown, 2012). Anomalies were interpolated between GCM cell centroids and were then applied to a baseline climate with a high-resolution (1km) surface.

https://doi.org/10.5194/essd-2021-53
Preprint. Discussion started: 24 March 2021

Open Access Earth System Science Data Discussions

3.3 Data Integration

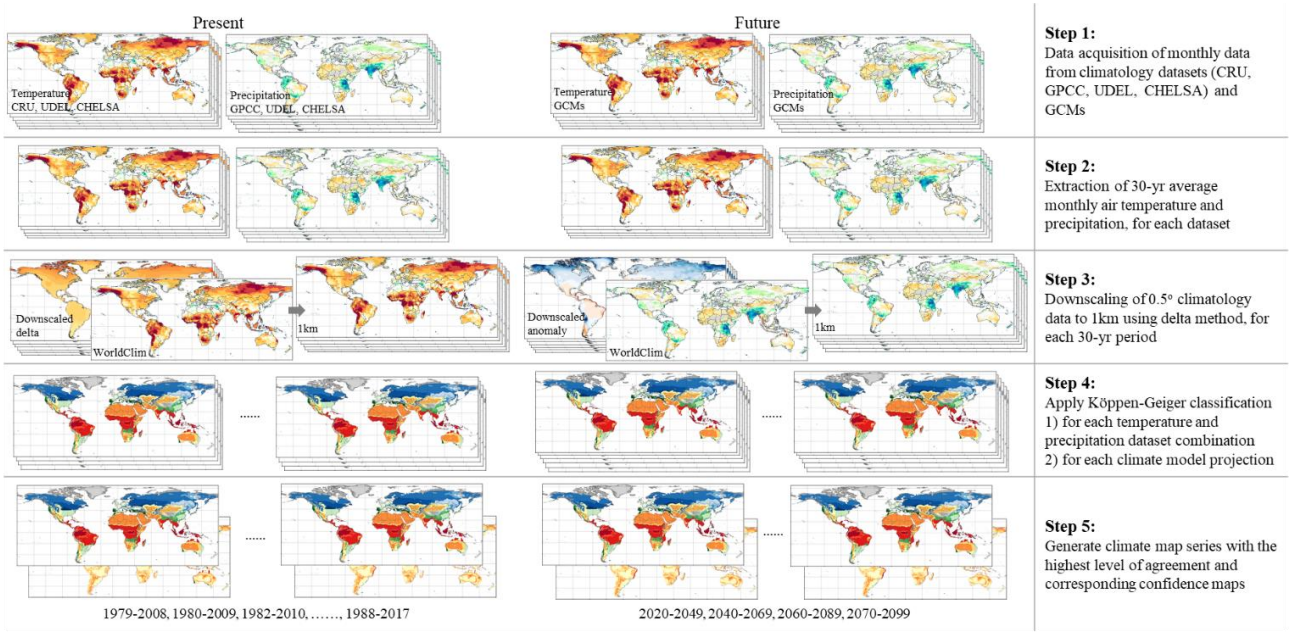

Figure 2. Step by step process to generate Köppen-Geiger climate map series.

The historical Köppen-Geiger climate classification map series was generated using the highest confidence class from an ensemble of maps using all combinations of surface air temperature and precipitation products (Fig. 2). The highest confidence was given to the most common climate class for each grid cell. The final historical climate map series were derived using the climate class with the highest level of confidence in an ensemble of 3 × 3 = 9 classification maps based on combinations of the 3 precipitation datasets (CRU, UDEL, and CHELSA) and 3 surface air temperature datasets (GPCC, UDEL, and CHELSA). To further test the sensitivity of the method using the climate with the highest level of agreement, we incorporated another data integration method using the mean of multiple datasets. To fully quantify the degree of confidence placed in the resulting Köppen-Geiger climate map series, we calculated the degree of confidence at the grid cell level by dividing the occurrence frequency of the climate class with the highest level of agreement by the ensemble size. The confidence level can be viewed as the degree of agreement in classification based on the multiple climatology datasets.

The future Köppen-Geiger climate classification map series under 4 RCPs, were derived based on the most common climate class from an ensemble of future climate maps. For each climate model projection, we generated a future Köppen-Geiger climate classification map with 1-km resolution using the CCAFS bias-corrected and downscaled CMIP5 GCM dataset. For example, the future Köppen-Geiger climate classification map series under RCP8.5 was derived from an ensemble of 30 maps based on 30 CMIP5 models. The level of confidence was estimated using the ratio between the frequency of the climate class with the highest level of agreement in the future map results, and the ensemble size.

https://doi.org/10.5194/essd-2021-53
Preprint. Discussion started: 24 March 2021

Open Access Earth System Science Data Discussions

4 Results and Discussion

4.1 Historical Köppen-Geiger climate maps

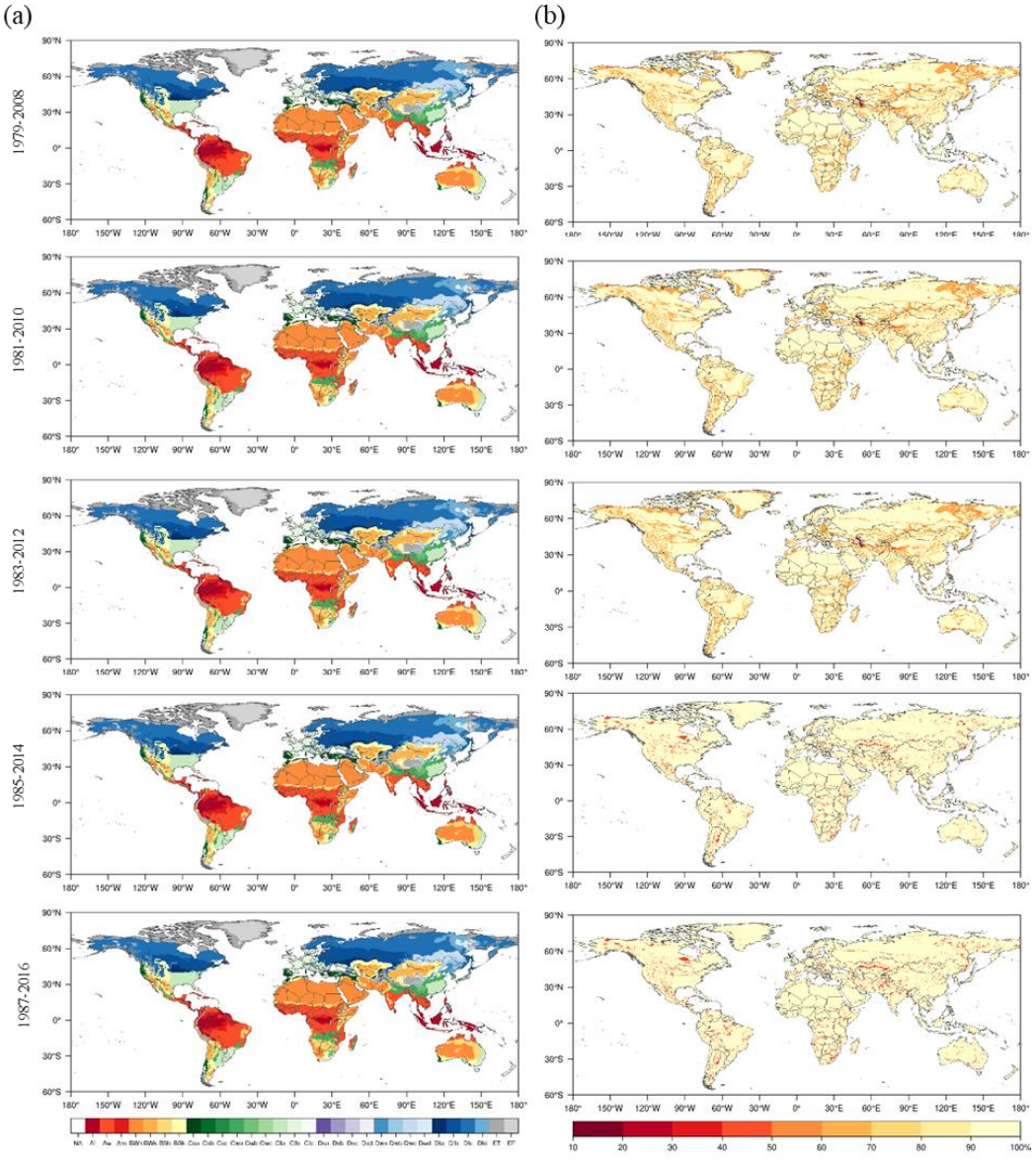

Figure 3 Global maps of Köppen-Geiger climate classification for the historical periods (1979-2008, 1981-2010, 1983-2012, 1985-2014, 1987-2016) and associated classification confidence levels. (a) Historical maps of Köppen-Geiger climate classification and (b) confidence levels associated with the Köppen-Geiger climate classification.

Global map series of Köppen-Geiger climate classification for historical periods and associated corresponding confidence levels are shown in Figure 3. Based on the distribution of confidence level, over 90% of the land area exhibit high level of confidence as classification results based on different climate data show excellent agreement. Relatively lower classification

https://doi.org/10.5194/essd-2021-53
Preprint. Discussion started: 24 March 2021

accuracy and large discrepancy in classification results are found especially in mountainous regions such as Andes Mountains, Rocky Mountains, Tibetan Plateau, and major climate transitional zones located in mid and high latitudes of Northern Hemisphere, Central Africa, and Central Asia.

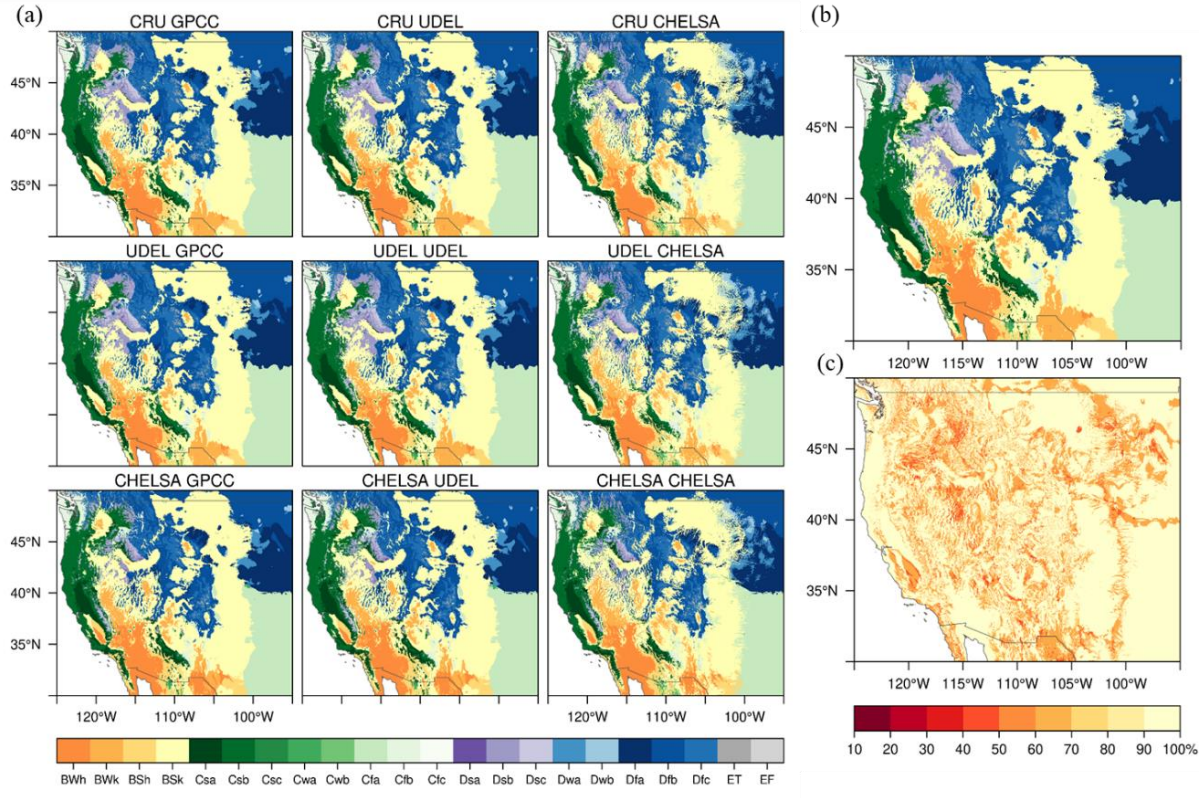

Figure 4. Present Köppen-Geiger classification and confidence map for 1979-2008 with resolution of 1km for the central Rocky Mountains in North America. (a) Climate maps based on the 9 combinations of the 3 precipitation datasets × 3 surface air temperature datasets, (b) the final climate map derived from the most common climate class among the 9 climate maps, and (c) confidence level distribution of the final climate map.

https://doi.org/10.5194/essd-2021-53
Preprint. Discussion started: 24 March 2021

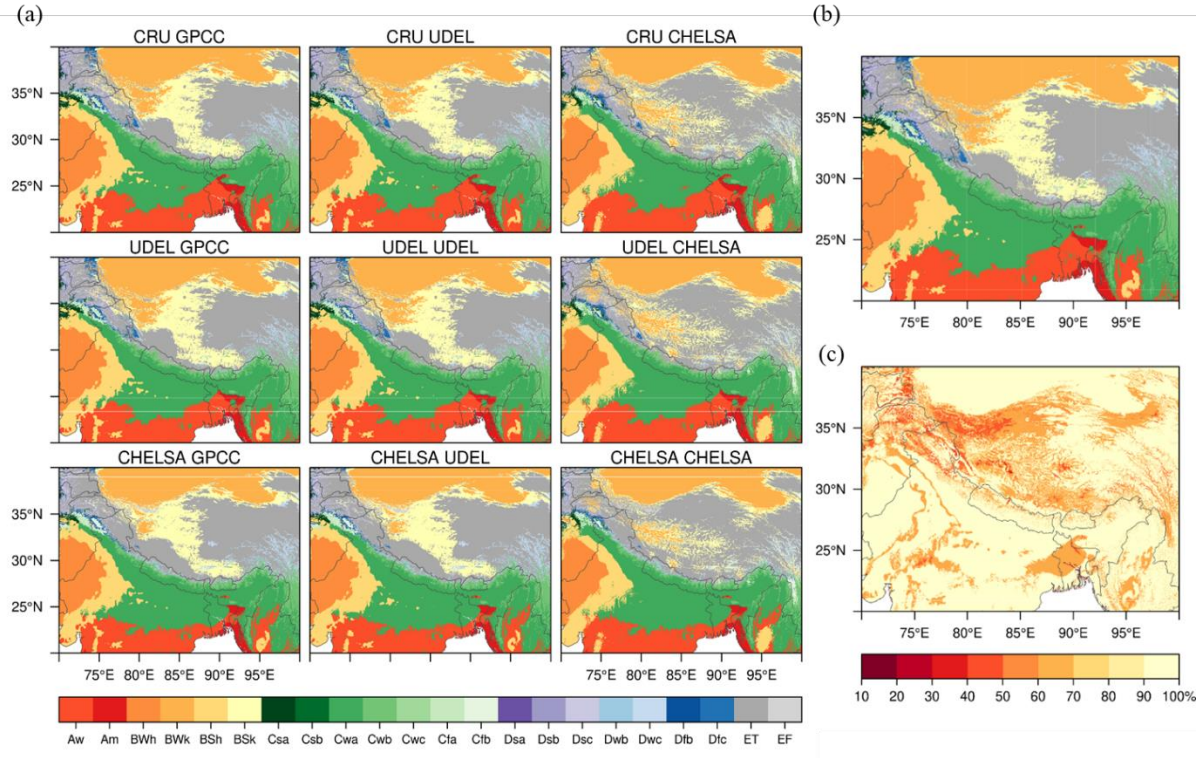

Figure 5. Present Köppen-Geiger classification and confidence map for 1979-2008 with resolution of 1km for the Tibetan Plateau. (a) Climate maps based on the 9 combinations of the 3 precipitation datasets × 3 surface air temperature datasets, (b) the final climate map derived from the most common climate class among the 9 climate maps, and (c) confidence level distribution of the final climate map.

Regional distributions of climatic conditions are largely created by local variation in topography in rugged terrain (Dobrowski et al., 2013; Franklin et al., 2013). The climate classification and confidence level maps of mountainous areas of Central Rocky Mountains and Tibetan Plateau are shown in Figure 4 and 5 respectively. For each combination of precipitation and surface air temperature datasets, we generated a Köppen-Geiger climate classification map (see Fig. 4a and 5a for 1979-2008 maps for the central Rocky Mountains and Tibetan Plateau). The final Köppen-Geiger classification map is derived based on the most common climate type among all the climate maps (Fig. 4b and 5b). We then calculated corresponding confidence levels to quantify the degree of uncertainty in the classification maps (Fig. 4c and 5c). The uncertainty in climate classification in mountainous areas is attributed to the uncertainty existing in climate data, especially precipitation data. In rugged terrain, CHELSA precipitation data shows more detailed precipitation patterns, causing disagreement in classificaion results of the 3rd level climate classes which depict precipitation seasonality.

https://doi.org/10.5194/essd-2021-53
Preprint. Discussion started: 24 March 2021

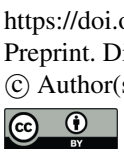

Open Access Earth System Science Data Discussions

235 **4.2 Future Köppen-Geiger climate maps**

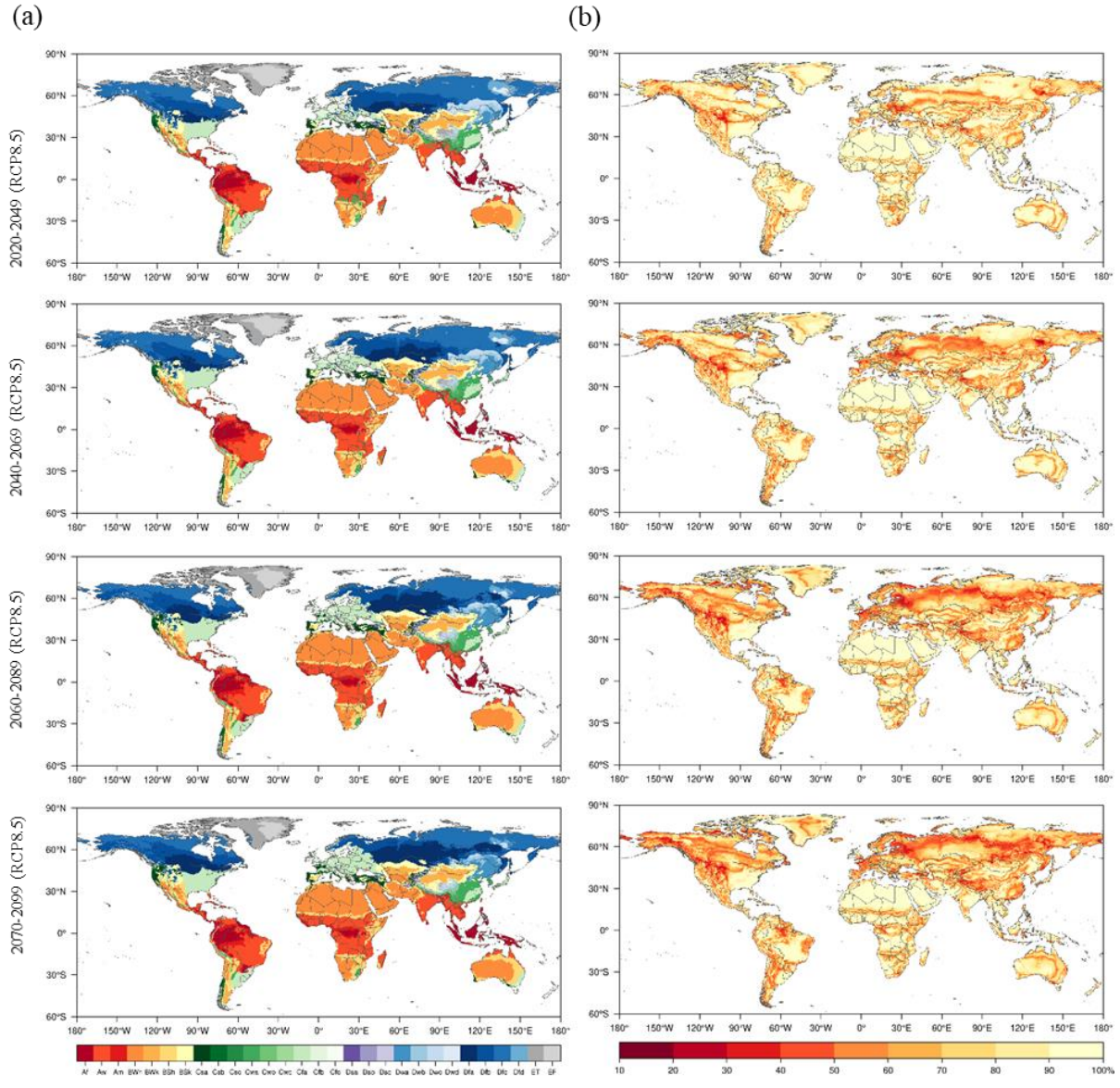

Figure 6 Global maps of Köppen-Geiger climate classification for the future periods (2020-2049, 2040-2069, 2060-2089, 2070-2099) under RCP8.5 and associated classification confidence levels. (a) Future maps of Köppen-Geiger climate classification and (b) confidence levels associated with the Köppen-Geiger climate classification.

240 Future Köppen-Geiger climate classification maps under RCP8.5 and associated confidence levels are shown in Figure 6. Indicated by confidence levels, there exist larger uncertainties in the final future climate maps than historical maps, particularly at mid and high latitudes. Climate map for the future period of 2070-2099 shows the largest uncertainty compared with the other future periods.

https://doi.org/10.5194/essd-2021-53
Preprint. Discussion started: 24 March 2021

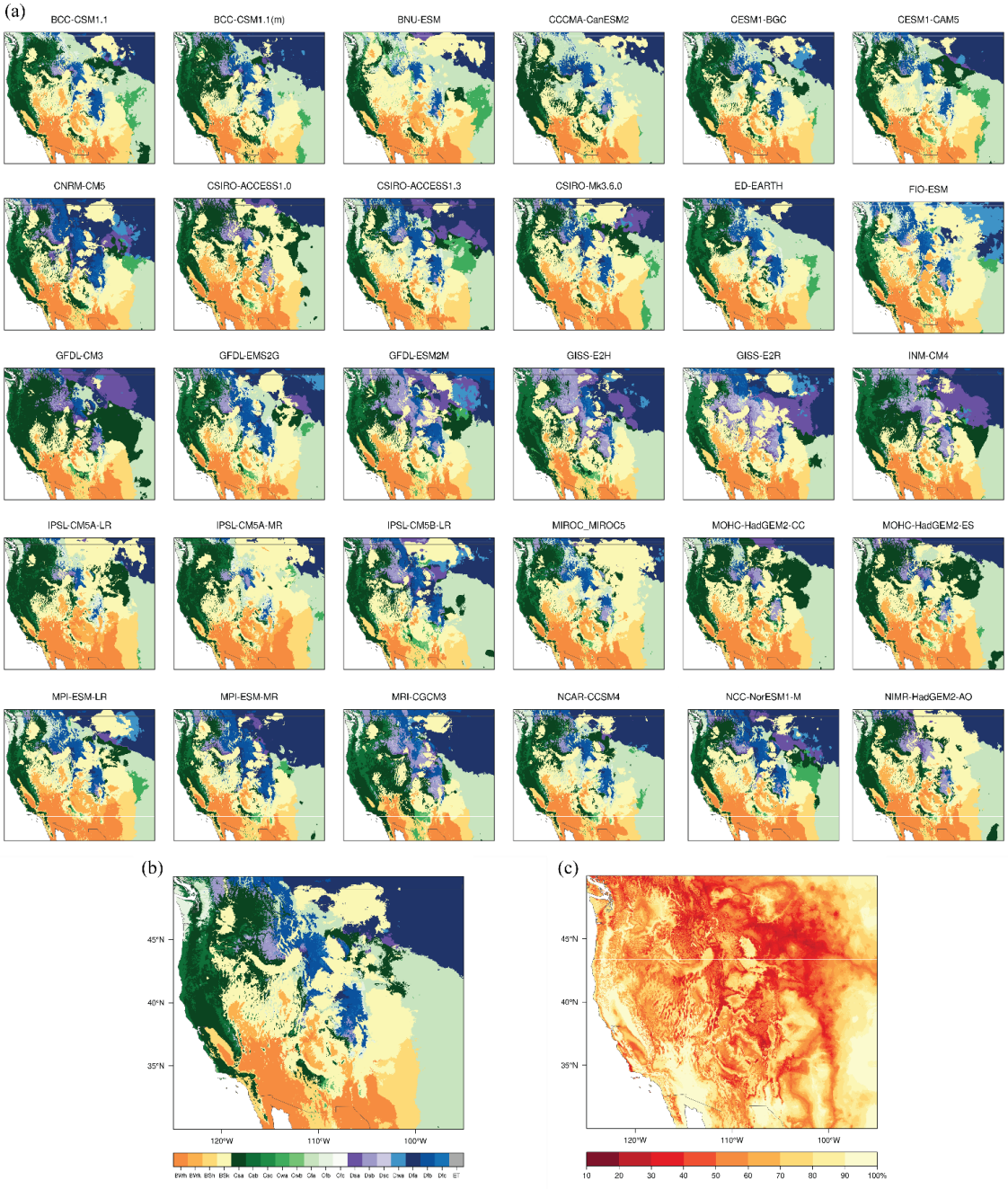

245 **Figure 7. Future Köppen-Geiger classification and confidence map for 2070-2099 under RCP8.5 with resolution of 1km for the central Rocky Mountains in North America.** (a) Climate maps based on 30 GCMs, (b) the final climate map derived from the most common climate class among all the 30 climate maps, and (c) confidence level distribution of the final climate map.

https://doi.org/10.5194/essd-2021-53
Preprint. Discussion started: 24 March 2021

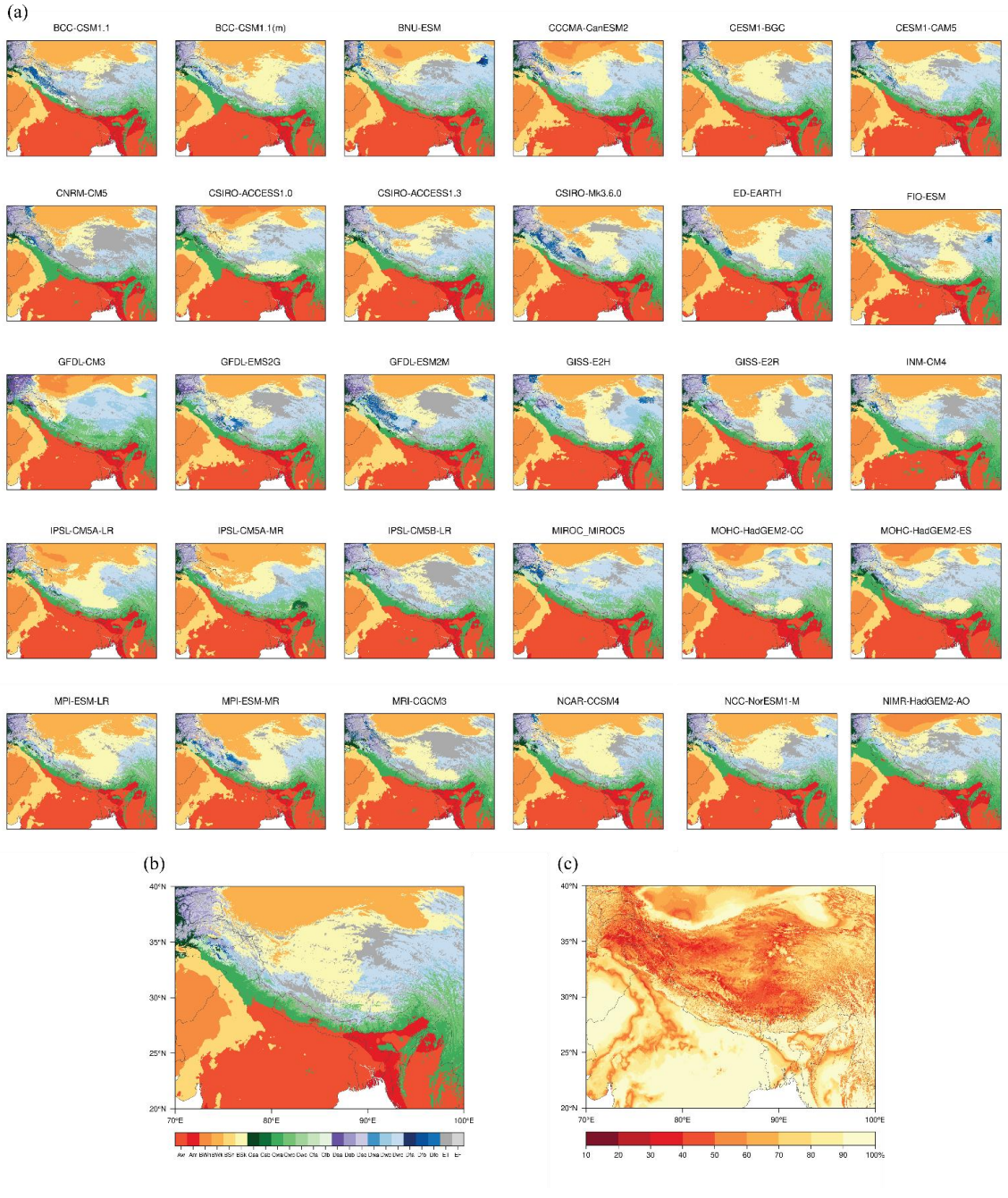

Figure 8. Future Köppen-Geiger classification and confidence map for 2070-2099 under RCP8.5 with resolution of 1km for the Tibetan Plateau. (a) Climate maps based on 30 GCMs, (b) the final climate map derived from the most common climate class among all the 30 climate maps, and (c) confidence level distribution of the final climate map.

Future climate classifications derived from the diverse GCM projections for four RCPs, which are inherently uncertain (Gleckler, Taylor, & Doutriaux, 2008; Winsberg, 2012), provide a proxy of global distributions of climatic conditions and can

https://doi.org/10.5194/essd-2021-53
Preprint. Discussion started: 24 March 2021

represent potential spatial changes in climate zones under global warming. The large uncertainty and strong disagreement in projected climate classification maps at high latitudes and in regions with rugged terrain can be indicated by relatively low confidence levels. Figure 7 and 8 show the future Köppen-Geiger climate classification maps based on GCM projections under RCP8.5 and associated confidence levels for the central Rocky Mountains and Tibetan Plateau. We generated a future Köppen-Geiger climate classification map for each bias-corrected and downscaled CMIP5 GCM projection (see Fig. 7a and 8a for 2070-2099 maps for the central Rocky Mountains and Tibetan Plateau). Noticeable regional changes in climate zones has been projected by comparing the 2070-2099 and 1979-2008 climate classification maps (see Fig. 4b and 7b for the central Rocky Mountains, and Fig. 5b and 8b for Tibetan Plateau).

https://doi.org/10.5194/essd-2021-53
Preprint. Discussion started: 24 March 2021

Open Access Earth System Science Data Discussions

4.3 Validation

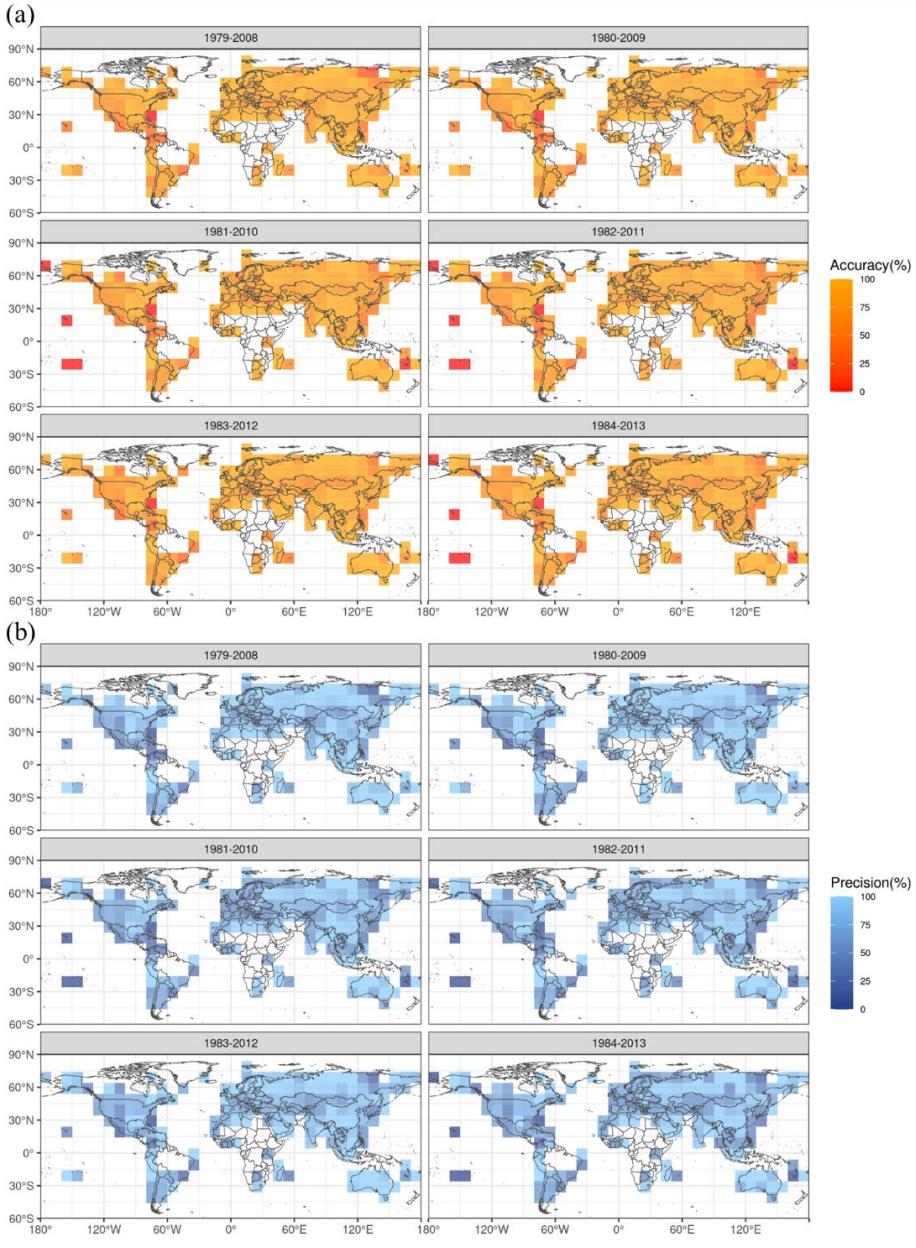

Figure 9. Validation of the historical Köppen-Geiger climate map series (1979-2008, 1980-2009, 1981-2010, 1982-2011, 1983-2012, 1984-2013). (a) Small-scale accuracy of historical Köppen-Geiger climate maps. (b) Small-scale precision of historical Köppen-Geiger climate maps. Climate classificaiton has been applied for each station. The small-scale accuracy and precision are calculated based on the classification results of all the stations within the given region, with a minimum of 3 stations in the 5° search radius.

https://doi.org/10.5194/essd-2021-53
Preprint. Discussion started: 24 March 2021

We validated the historical climate maps using the station observations from Global Historical Climatology Network-Daily (GHCN-D) (Menne et al., 2012) and Global Summary Of the Day (GSOD) database (National Climatic Data Center et al., 2015) as reference data. For each station, time series of monthly temperature and precipitation were calculated from the daily observations with months with <15 daily values discarded. Then if ⩾6 months are present, monthly climatology were generated subsequently by averaging the monthly means for the given period, typically 30 years. We discarded stations with gap years or missing data in the given 30 years. For each station and each 30-yr period, we applied Köppen-Geiger climate classification. We evaluated overall classification performance for each climate map using total accuracy, which is defined as the percentage of correct classes, and average precision, which is averaged fraction of correct classification for all climate classes. Figure 9 shows the small-scale distributions of total accuracy and average precision for historical Köppen-Geiger climate map series with 10° grid cells. Due to uneven distributions of weather stations, remote areas in the Pacific islands, Central Africa, and Amazon Forest suffer from a lack of station observations or an underrepresented validation results. Overall, the spatial patterms of total accuracy and average precision show good correspondence with classification confidence levels, indicating a potential of confidence level to represent classification uncertainty.

4.4 Sensitivity analysis

Table 3 Accuracy of the 1km Köppen-Geiger climate map series derived from different combinations of temperature and precipitation dataset input, and by different means of integration of multiple datasets. The values represent overall accuracy based on the technical validation using ground observation as reference.

Temperature	CHELSA, Downscaled CRU and UDEL		Downscaled CRU and UDEL		CHELSA
Precipitation	CHELSA, Downscaled GPCC and UDEL		Downscaled GPCC and UDEL		CHELSA
Integration of multiple datasets	Highest level of agreement	Mean of multiple datasets	Highest level of agreement	Mean of multiple datasets	-
1979-2008	83.25%	83.66%	83.13%	83.33%	79.72%
1980-2009	82.96%	83.44%	82.74%	82.78%	79.14%
1981-2010	82.63%	82.86%	81.95%	82.38%	78.03%
1982-2011	82.42%	82.73%	81.93%	82.11%	78.47%
1983-2012	81.48%	82.34%	81.14%	81.49%	78.32%
1984-2013	81.62%	82.05%	80.84%	81.27%	78.26%
1985-2014	-	-	80.23%	80.86%	-
1986-2015	-	-	79.79%	80.58%	-
1987-2016	-	-	78.76%	79.62%	-
1988-2017	-	-	-	78.65%	-
Average	82.39%	82.85%	81.17%	81.31%	78.66%
1980-2017 (Beck et al. 2018)	77.65%				

https://doi.org/10.5194/essd-2021-53
Preprint. Discussion started: 24 March 2021

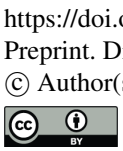

Open Access Earth System Science Data Discussions

We tested sensitivity of the climate map series using different combinations of temperature and precipitation dataset, and different method of data integration (Table 3). Results indicated an average total accuracy of the 1km Köppen-Geiger classification maps generated with all the CHELSA, donwscaled CRU, GPCC and UDEL datasets and with only downscaled CRU, GPCC, UDEL datasets as 82.39% and 81.17% respecively. Using the mean of multiple datasets which can potentially reduce the data bias, led to better classification results. Compared with the recently published Köppen-Geiger climate map product, Beck et al. (2018), the newly generated Köppen-Geiger climate map series showed greater accuracy in total.

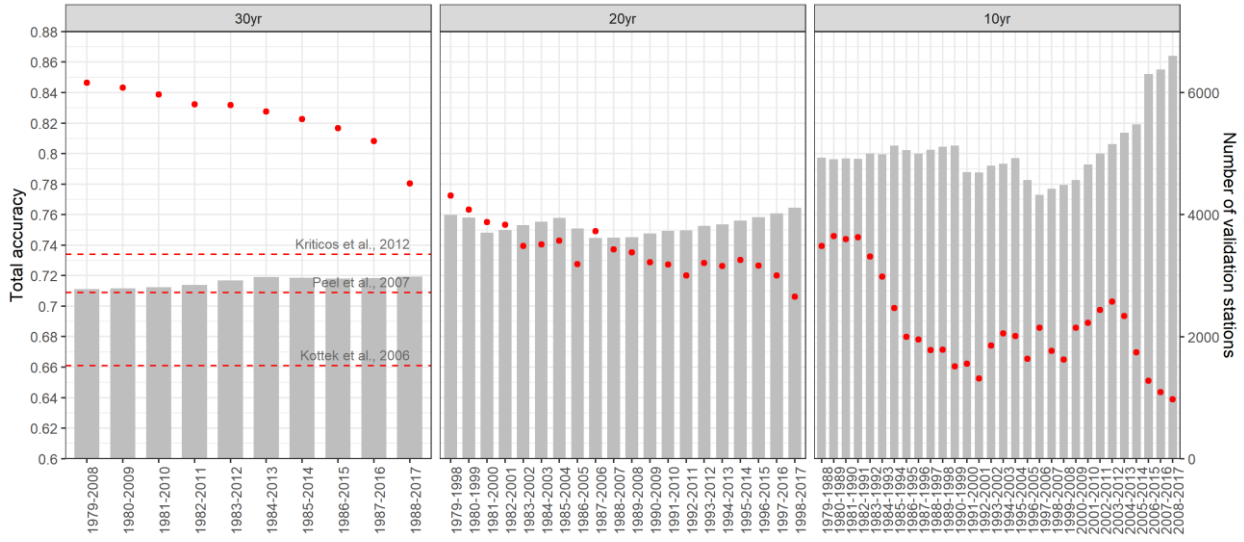

Figure 10. Validation of downscaled data of bioclimatic variables and the generated Köppen-Geiger climate map.

We conducted sensitivity analysis of the Köppen classification scheme and tested multiple time scales, 10-yr, 20-yr, and 30-yr. The selection criteria of station observations were adjusted accordingly based on the time scale utilized. Duplicate stations in the two datasets were further removed. Accuracy results exhibited decreasing accuracy for shorter time scale (Fig. 10). Further, we estimated the total accuracy for Köppen-Geiger climate classification maps from previous studies, Beck et al., (2018) Kriticos et al., (2012), Peel et al., (2007), and Kottek et al., (2006), using the same validation dataset and consistent Köppen-Geiger climate classification scheme the corresponding study applied. The validation results demonstrate that the new Köppen-Geiger maps have comparatively higher overall accuracy than all the previous studies.

https://doi.org/10.5194/essd-2021-53
Preprint. Discussion started: 24 March 2021

Open Access Earth System Science Data Discussions

4.5 Regional and continental scale comparison

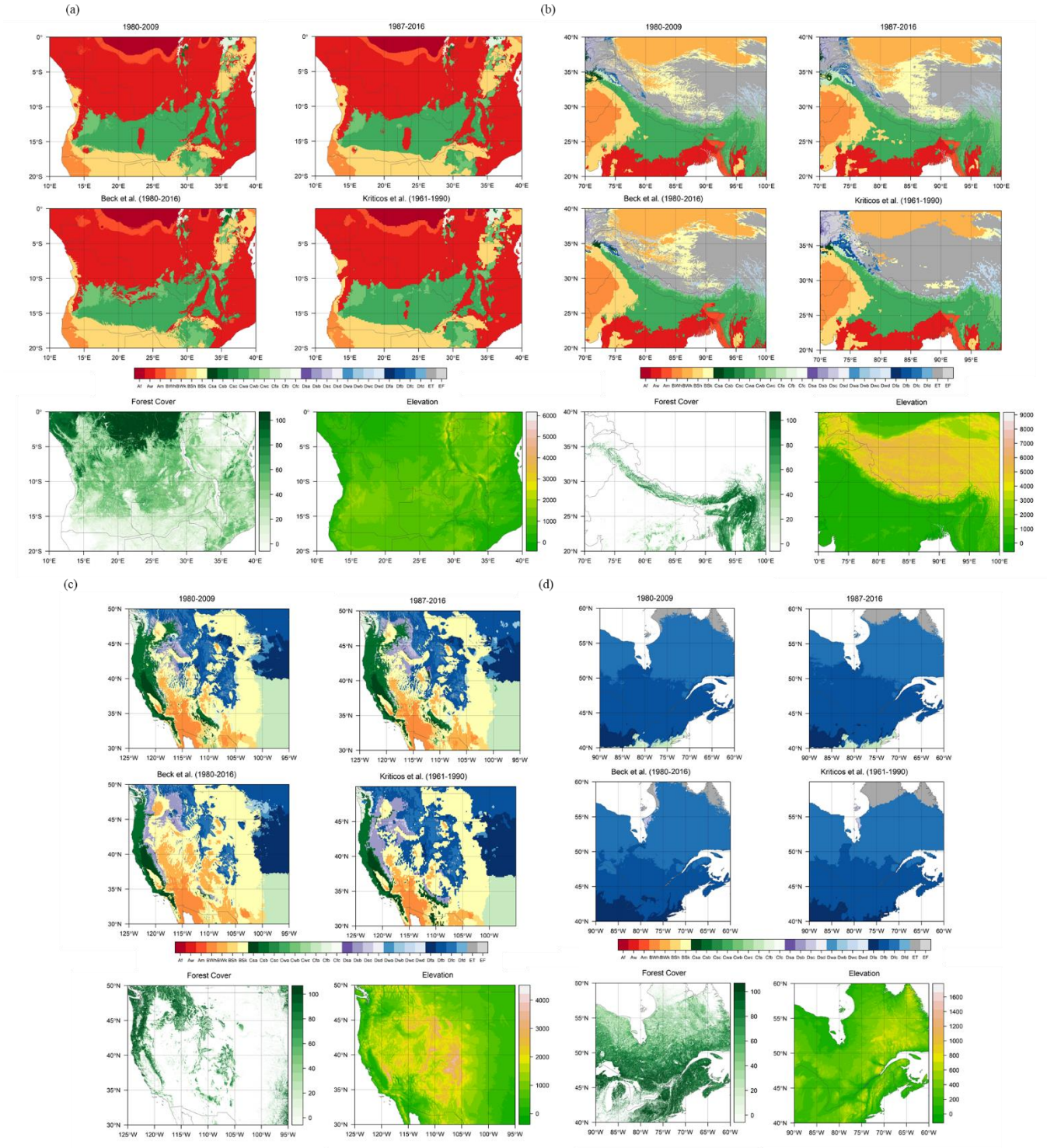

https://doi.org/10.5194/essd-2021-53
Preprint. Discussion started: 24 March 2021

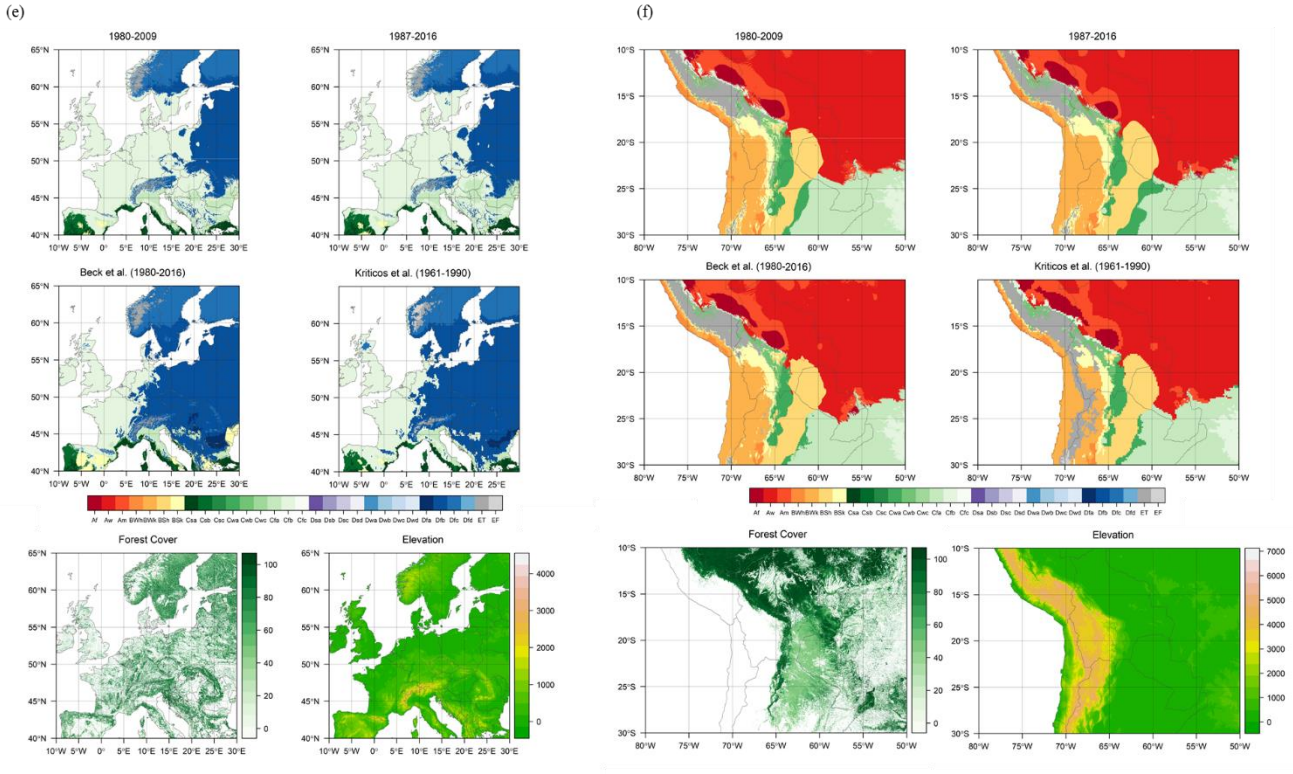

Figure 11. Köppen-Geiger climate classification maps from our study and previous studies, Beck et al., 2018, and Kriticos et al., 2012, associated forest cover and elevation maps, for regions with large spatial gradients in climates or sharp elevation gradients. (a) Central and eastern Africa, (b) Tibetan Plateau, (c) central Rocky Mountains, (d) high latitudes in North America, (e) Europe, and (f) central Andes. The forest cover map is the 30m Landsat-based forest cover map for year 2000 (Hansen et al., 2013). The elevation data is the NASA SRTM Digital Elevation 30m data (Farr et al., 2007). The representative period of each map is listed in parentheses.

At the regional and continental scale, we compared our Köppen-Geiger climate classification maps with previous map products for regions with large spatial gradients in climates, including central and eastern Africa, Europe, North America, and regions with sharp elevation gradients, including Tibetan Plateau, central Rocky Mountains, central Andes. The high-resolution Köppen-Geiger maps from two previous studies, Beck et al., (2018), and Kriticos et al., (2012) are used to evaluate the new Köppen-Geiger climate classification maps. To show the agreement between the improved Köppen-Geiger climate classification maps and regional lanscape distributions, we showed maps of forest cover, and elevation distribution for these regions. The forest cover map we used is the 2000 30m Landsat-based forest cover map (Hansen et al., 2013). The elevation is from the NASA SRTM Digital Elevation 30m data (Farr et al., 2007). Figure 11 illustrate the enhanced regional details of the maps.

Compared with Köppen-Geiger climate maps from previous studies, the series of Köppen-Geiger climate maps from our study demonstrate the ability to capture recent changes in spatial distributions of climate zones. Changes in climate zones have been the most significant since the 1980s because, climate zone changes specifically, changes in arid (B) ans polar (E) climate

https://doi.org/10.5194/essd-2021-53
Preprint. Discussion started: 24 March 2021

zones, are highly susceptible to the accelerated global warming since the 1980s (Cui, Liang, & Wang, 2021). Another improvement of the new series of Köppen-Geiger climate maps is the application of threshold of -3 ºC as the boundary of temperate (C) and boreal (D) climate zones, which show better agreement with global boreal forest distributions compared with Russell's modification of 0 ºC (1931), which Beck et al., (2018), and Kriticos et al., (2012) utilized. Moreover, the new Köppen-Geiger maps show accurate depiction of important topographic features and correspond closely with tree lines in the forest cover maps over the regions with complex topography (Fig. 11).

4.6 Bioclimatic variables

Table 4 List of bioclimatic variables derived from downscaled monthly climate data.

Bioclimatic Variables	Description
BIO1	Annual mean temperature (ºC)
BIO2	Temperature of the warmest month (ºC)
BIO3	Temperature of the coldest month (ºC)
BIO4	Annual precipitation (mm)
BIO5	Precipitation of the warmest half year (mm)
BIO6	Precipitation of the coldest half year (mm)
BIO7	Precipitation of the driest month (mm)
BIO8	Precipitation of the driest month in the warmest half year (mm)
BIO9	Precipitation of the driest month in the coldest half year (mm)
BIO10	Precipitation of the wettest month (mm)
BIO11	Precipitation of the wettest month in the warmest half year (mm)
BIO12	Precipitation of the wettest month in the coldest half year (mm)

Beyond the Köppen-Geiger climate classification maps, we calculated a set of bioclimatic variables from the monthly climate data (see full list in Table 4). The bioclimatic variables at 1-km sptial resolution can capture regional environmental variations expecially in mountainous areas and areas with steep climate gradients. These bioclimatic variables can be used in studies of environmental, agricultural and biological sciences, for example, development of species distribution modelling and assessment of biological impacts induced by climate change. The variables provide descriptions of annual averages, and seasonality of climates. The warmest half year or the coldest half year is defined as the period of the warmest six months or the coldest six months.

https://doi.org/10.5194/essd-2021-53
Preprint. Discussion started: 24 March 2021

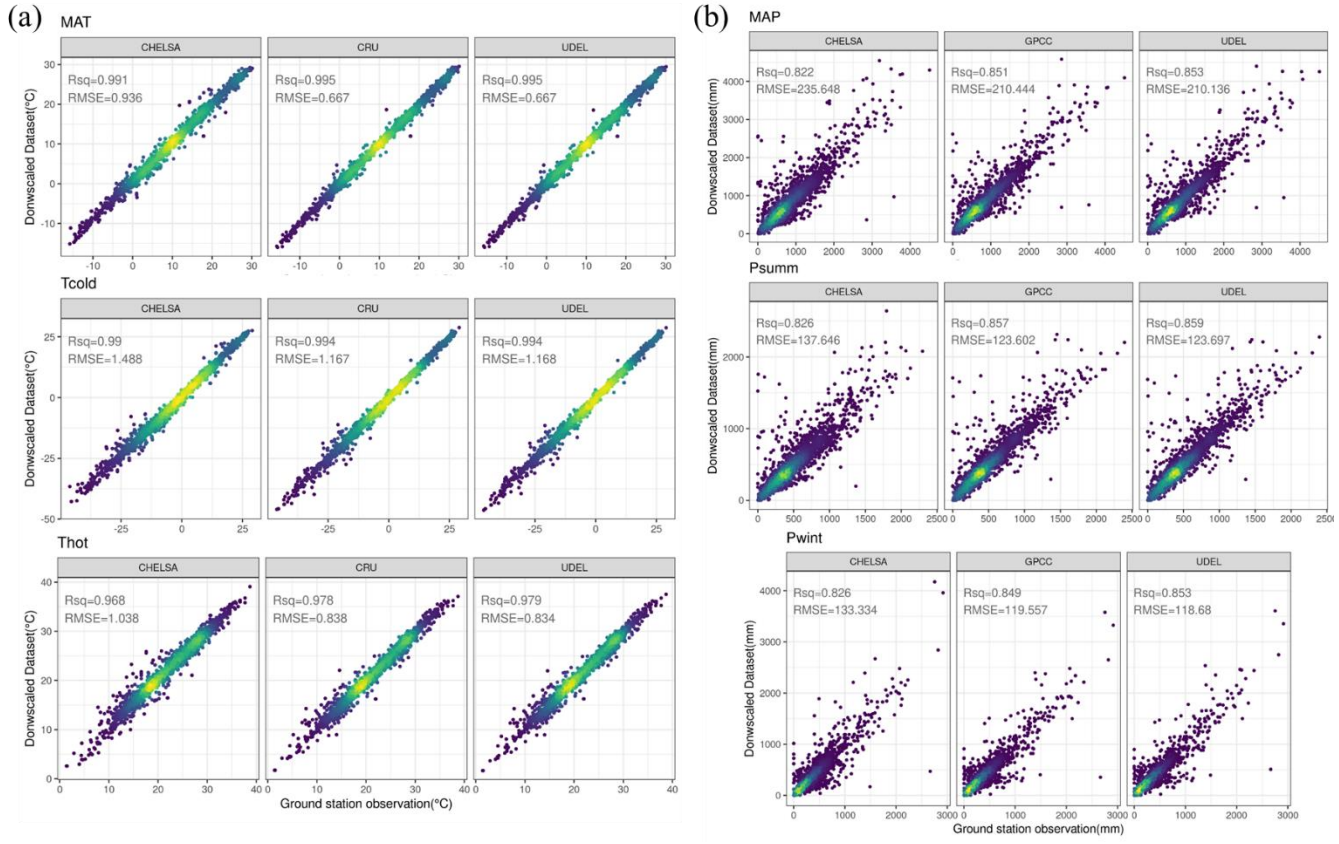

Figure 12. Scatter plots of the station observations and estimates of bioclimatic variables from downscaled climatology data. The bioclimatic variables include the 30-yr means of annual temperature (MAT), the air temperature of the coldest month (Tcold), the air temperature of the warmest month (Thot), total annual precipitation (MAP), precipitation of the summer half year (Psumm), and precipitation of the winter half year (Pwint). (a) Scatter plots of the station observations and downscaled temperature data from CHELSA, CRU, UDEL datasets, and (b) and downscaled precipitation data from CHELSA, GPCC, UDEL datasets.

We validated the bioclimatic variables from different datasets with station data from GHCN-D (Menne et al., 2012) and GSOD database (National Climatic Data Center et al., 2015) (Fig. 12). We calculated a linear regression model for the 12 bioclimatic variables for each 10° grid cell (Fig. 13). The 30-yr average mean annual temperature (MAT) from CHELSA dataset shows overall highest fit with station data, with CRU, and UDEL datasets showing smaller, but still strong correlation with station data. The 30-yr average mean annual precipitation (MAP) estimates from GPCC, UDEL, and CHELSA datasets have considerable uncertainties, indicated by relatively low correlation with station observations. In current precipitation datasets, there exist a varied degree of discrepancy in annual estimates over multiple time scales (Sun et al., 2018).

https://doi.org/10.5194/essd-2021-53
Preprint. Discussion started: 24 March 2021

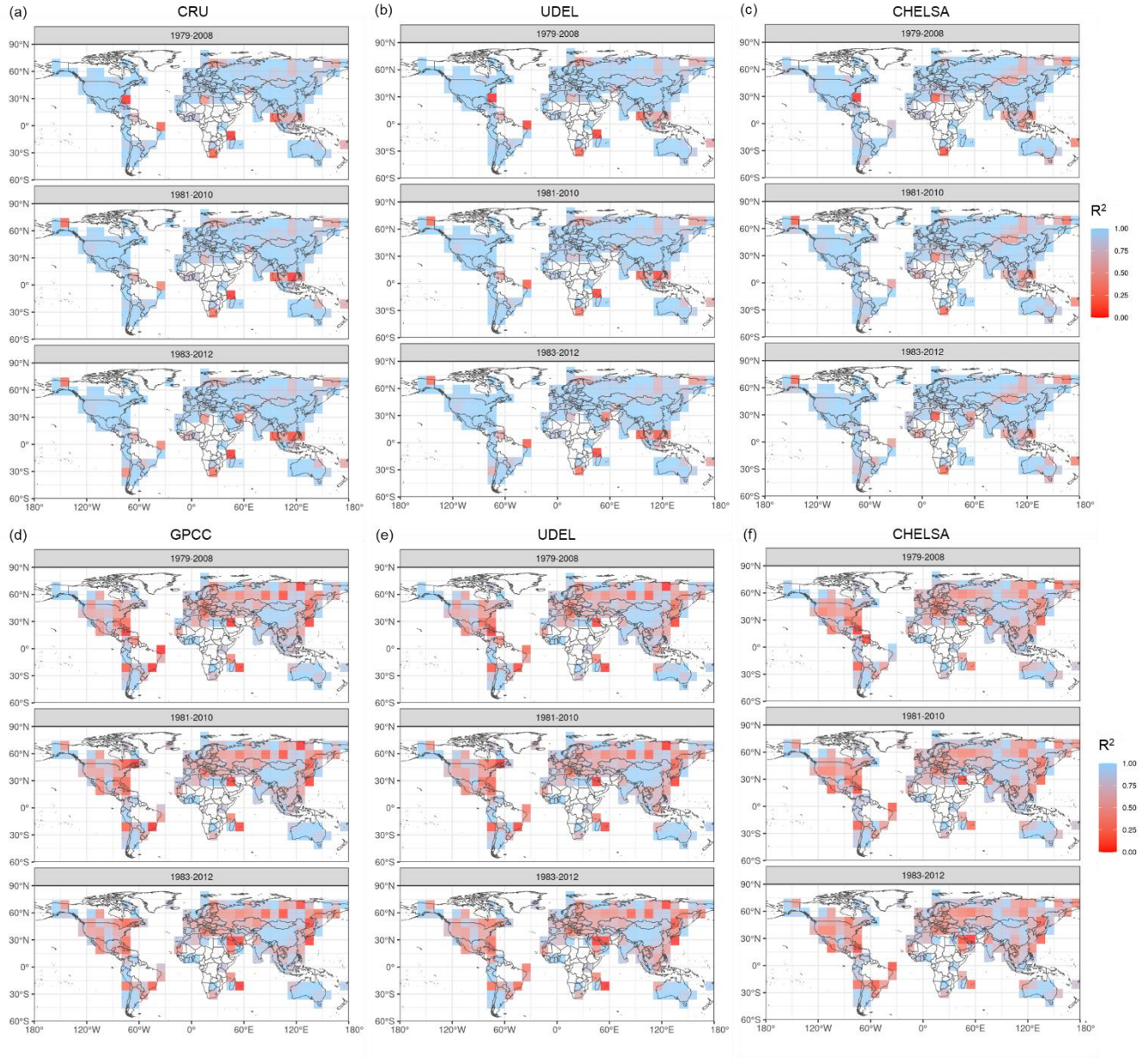

Figure 13. Small-scale comparison of annual temperature (MAT) and mean annual precipitation (MAP) variables derived from different datasets with station data. Small-scale correlation between the 30-yr average mean annual temperature (MAT) and mean annual precipitation (MAP) data and ground observations for three historical periods (1979-2008, 1981-2010, 1983-2012). The station data is from GHCN-D and GSOD database. The figure shows the R^2 value for 10° grid cells. (a), (b), and (c) are MAT results. (d), (e), and (f) are MAP results. (a) MAT is calculated from downscaled monthly temperature data from CRU dataset, (b) from UDEL dataset and (c) from CHELSA dataset. (d) MAP is calculated from downscaled monthly precipitation data from GPCC dataset, (e) from UDEL dataset and (f) from CHELSA dataset.

https://doi.org/10.5194/essd-2021-53
Preprint. Discussion started: 24 March 2021

Open Access Earth System Science Data Discussions

355 **4.7 Application example: detection of area changes in climate zones**

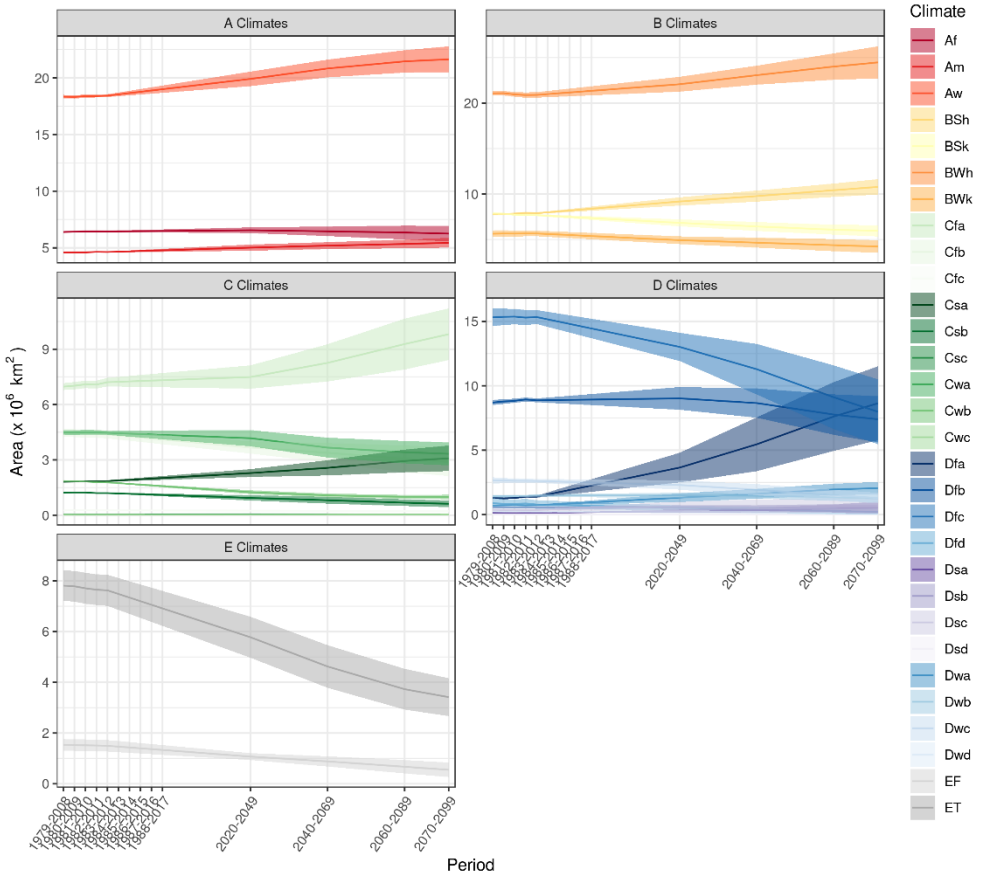

Figure 14. Area changes in climate zones since the 1980s on a global scale under RCP8.5. The error bars for historical periods (1979-2017) indicate standard error in the Köppen-Geiger classification results based on the 9 combinations of observational air temperature and precipitation datasets and for future periods (2020-2099), the error bars indicate standard error in the Köppen-Geiger classification results
360 based on the 30 GCMs.

Changes in climatic conditions under global warming have significant impacts on biodiversity and ecological systems. Area changes of climate zones can indicate spatial shrinkage or expansion of analogous climatic conditions, potentially implying threats for species range contraction or opportunities for range expansion (Cui, Liang, & Wang, 2021). To examine the area changes of climate zones, we calculated the total area covered by each climate type for each historical and future periods
365 under high-emission RCP8.5 scenario (Fig. 14). Results show that accelerated anthropogenic global warming since the 1980s has caused large-scale changes in climate zones and the shifts into warmer and drier climates are projected in this century. The tropical and arid climates are expanding into large areas in mid latitudes whereas the high-latitude climates will experience significant area shrinkage.

https://doi.org/10.5194/essd-2021-53
Preprint. Discussion started: 24 March 2021

5 Conclusion

Changes in broad-scale climatic conditions, driven by anthropogenic global warming, lead to the redistribution of species diversity and the reorganization of ecosystems. Distributions of the Earth's climatic conditions are widely described based on the climate zones characterized following the Köppen climate classification system. Most of the current Köppen climate classification world maps, especially the ones published in early years, have a relatively low resolution of 0.5° (Cui, Liang, & Wang, 2021). Fine resolutions of at least 1-km are required to detect relevant microrefugia and promote effective conservation. Moreover, single or non-comparable period coverage (Beck et al., 2018) may not sufficiently fulfil the current research needs. There exists an urgent need to compile a series of global maps of Köppen climate classification with finer spatial and temporal resolutions, and improved accuracy.

We presented an improved long-term Köppen-Geiger climate classification map series for ten historical 30-yr periods in 1979-2017 and four future 30-yr periods in 2020-2099 under RCP2.6, 4.5, 6.0 and 8.5. To improve the classification accuracy and achieve a resolution as fine as 1-km, we combined multiple datasets, including WorldClim V2, CHELSA V1.2, CRU TS v4.03, UDEL, GPCC datasets and bias-corrected downscaled CMIP5 model simulations from CCAFS. The historical climate maps are based on the most common climate type from an ensemble of climate maps derived from combinations of observational climatology datasets. The future climate maps are based on an ensemble of climate maps derived from 35 GCMs. We estimated the corresponding confidence levels to quantify the uncertainty in climate maps. We also calculated 12 bioclimatic variables at the same 1-km resolution using these climate datasets for the same historical and future periods to provide data of annual averages, seasonality, and stressful conditions of climates.

To validate the Köppen-Geiger climate classification maps, we used the station observations from GHCN-D and GSOD database. Our validation results show that the new Köppen-Geiger maps have comparatively higher overall accuracy than all the previous studies. Although the new maps exhibit improved overall accuracy, relatively lower confidence level and larger discrepancy in classification results are found especially in mountainous regions and major climate transitional zones located in mid and high latitudes. The confidence levels can provide a useful quantification of classification uncertainty.

Compared with climate maps from previous studies with a single present-day period, the series of Köppen-Geiger climate maps from our study demonstrate the ability to capture recent and future projected changes in spatial distributions of climate zones. On regional and continental scale, the new maps show accurate depictions of topographic features and correspond closely with vegetation distributions. However, we should take cautions when relating the changes to changes in actual biome distributions. Vegetation changes may lag the climate changes when climate become less favourable. Additionally, other factors not considered in the Köppen classification scheme, such as CO_2 or nitrogen levels, may influence the relationship between climate and vegetation. We should view the Köppen-Geiger climate classificaion as a descriptive and ecological relevant way which can provide insights into spatial distributions of climate zones.

Another limitation is that the future of Köppen-Geiger climate maps built on dowscaled climate model projections exsit unaviodable uncertainties. The classification agreement levels of GCMs are relatively low at high latitudes and in regions with

https://doi.org/10.5194/essd-2021-53
Preprint. Discussion started: 24 March 2021

rugged terrain. The main sources of model discrepancies and uncertainties are deficiencies in model physics and varied model resolution. The climate model outputs have coarse spatial resolution varying from 70-400 km and cannot well represent future climate change at the same scale of 1-km as our baseline climatology. Through bias-corretion and donwscaling methods, we made assumptions that local relationships between climatic variables remain constant across different scales, leading to a compromise between spatial scale and climate model physics.

We also tested the sensitivity of classification results to different time scale, dataset input, and data integration methods. Results show that 30-yr time scale exhibited the highest accuacy results. Moreover, using the mean of multiple datasets from CHELSA, CRU, UDEL, and GPCC could lead to better classification results. Last, we provided a heuristic example which used climate classification map series to detect the long-term area changes of climate zones, showing how the new Köppen-Geiger climate classification map series can be applied in climate change studies. With improved accuracy, high spatial resolution, long-term continuous time coverage, this global dataset of Köppen-Geiger climate classification and bioclimatic variables can be used to in conjunction with species distribution models to promote biodiversity conservation, and to analyse and identify recent and future interannual or interdecadal changes in climate zones on a global or regional scale.

Data Availability

This high-resolution global dataset of Köppen-Geiger climate classification and bioclimatic variables dataset for historical periods in 1979-2017 is available at http://doi.org/10.5281/zenodo.4546140 (Cui, Liang, Wang, & Liu, 2021b). The dataset for future periods in 2020-2100 is available at http://doi.org/10.5281/zenodo.4542076 (Cui, Liang, Wang, & Liu, 2021a).

Author Contribution

C.D. designed the computational framework, performed data collection and processing, conducted validation and sensitivity analyses, and wrote the manuscript. L.Z. contributed to the data processing. L.S. was involved in planning and supervised the work. All authors discussed the results and commented on the manuscript.

Competing Interests

The authors declare that they have no conflict of interest.

References

Beck, C., Grieser, J., & Rudolf, B. (2005). A new monthly precipitation climatology for the global land areas for the period 1951 to 2000. *Klimastatusbericht KSB, 2004*.

https://doi.org/10.5194/essd-2021-53
Preprint. Discussion started: 24 March 2021

Beck, H. E., Zimmermann, N. E., McVicar, T. R., Vergopolan, N., Berg, A., & Wood, E. F. (2018). Present and future Köppen-Geiger climate classification maps at 1-km resolution. *Scientific Data*, *5*, 180214. https://doi.org/10.1038/sdata.2018.214

Belda, M., Holtanová, E., Halenka, T., & Kalvová, J. (2014). Climate classification revisited: From Köppen to Trewartha. *Climate Research*, *59*(1), 1–13. https://doi.org/10.3354/cr01204

Belda, M., Holtanová, E., Kalvová, J., & Halenka, T. (2016). Global warming-induced changes in climate zones based on CMIP5 projections. *Climate Research*, *71*(1), 17–31. https://doi.org/10.3354/cr01418

Bockheim, J. G., Gennadiyev, A. N., Hammer, R. D., & Tandarich, J. P. (2005). Historical development of key concepts in pedology. *Geoderma*, *124*(1-2), 23–36. https://doi.org/10.1016/j.geoderma.2004.03.004

Brugger, K., & Rubel, F. (2013). Characterizing the species composition of European Culicoides vectors by means of the Köppen-Geiger climate classification. *Parasites & Vectors*, *6*(1), 333. https://doi.org/10.1186/1756-3305-6-333

Chan, D., & Wu, Q. (2015). Significant anthropogenic-induced changes of climate classes since 1950. *Scientific Reports*, *5*, 13487. https://doi.org/10.1038/srep13487

Chen, D., & Chen, H. W. (2013). Using the Köppen classification to quantify climate variation and change: An example for 1901-2010. *Environmental Development*, *6*, 69–79. https://doi.org/10.1016/j.envdev.2013.03.007

Chen, I.-C., Hill, J. K., Ohlemüller, R., Roy, D. B., & Thomas, C. D. (2011). Rapid range shifts of species associated with high levels of climate warming. *Science (New York, N.Y.)*, *333*(6045), 1024–1026. https://doi.org/10.1126/science.1206432

Chen, M., Xie, P., Janowiak, J. E., & Arkin, P. A. (2002). Global land precipitation: A 50-yr monthly analysis based on gauge observations. *Journal of Hydrometeorology*, *3*(3), 249–266.

Craven, P., & Wahba, G. (1978). Smoothing noisy data with spline functions. *Numerische Mathematik*, *31*(4), 377–403. https://doi.org/10.1007/BF01404567

Cui, D., Liang, S., & Wang, D. (2021). Observed and projected changes in global climate zones based on Köppen climate classification. *Wiley Interdisciplinary Reviews: Climate Change*, e701. https://doi.org/10.1002/wcc.701

Cui, D., Liang, S., Wang, D., & Liu, Z. (2021a). KGClim future: A 1-km global dataset of future (2020-2100) Köppen-Geiger climate classification and bioclimatic variables (Version V1). Advance online publication. https://doi.org/10.5281/zenodo.4542076

Cui, D., Liang, S., Wang, D., & Liu, Z. (2021b). KGClim historical: A 1-km global dataset of historical (1979-2017) Köppen-Geiger climate classification and bioclimatic variables (Version V1). Advance online publication. https://doi.org/10.5281/zenodo.4546140

https://doi.org/10.5194/essd-2021-53
Preprint. Discussion started: 24 March 2021

Dobrowski, S. Z., Abatzoglou, J., Swanson, A. K., Greenberg, J. A., Mynsberge, A. R., Holden, Z. A., & Schwartz, M. K. (2013). The climate velocity of the contiguous United States during the 20th century. *Global Change Biology*, *19*(1), 241–251. https://doi.org/10.1111/gcb.12026

Fan, Y., & Dool, H. v. d. (2008). A global monthly land surface air temperature analysis for 1948–present. *Journal of Geophysical Research*, *113*(D1), 161. https://doi.org/10.1029/2007JD008470

Farr, T. G., Rosen, P. A., Caro, E., Crippen, R., Duren, R., Hensley, S., . . . Alsdorf, D. (2007). The Shuttle Radar Topography Mission. *Reviews of Geophysics*, *45*(2), 1485. https://doi.org/10.1029/2005RG000183

Feng, S., Ho, C.-H., Hu, Q., Oglesby, R. J., Jeong, S.-J., & Kim, B.-M. (2012). Evaluating observed and projected future climate changes for the Arctic using the Köppen-Trewartha climate classification. *Climate Dynamics*, *38*(7-8), 1359–1373. https://doi.org/10.1007/s00382-011-1020-6

Feng, S., Hu, Q., Huang, W., Ho, C.-H., Li, R., & Tang, Z. (2014). Projected climate regime shift under future global warming from multi-model, multi-scenario CMIP5 simulations. *Global and Planetary Change*, *112*, 41–52. https://doi.org/10.1016/j.gloplacha.2013.11.002

Fick, S. E., & Hijmans, R. J. (2017). WorldClim 2: New 1-km spatial resolution climate surfaces for global land areas. *International Journal of Climatology*, *37*(12), 4302–4315. https://doi.org/10.1002/joc.5086

Franke, R. (1982). Smooth interpolation of scattered data by local thin plate splines. *Computers & Mathematics with Applications*, *8*(4), 273–281. https://doi.org/10.1016/0898-1221(82)90009-8

Franklin, J., Davis, F. W., Ikegami, M., Syphard, A. D., Flint, L. E., Flint, A. L., & Hannah, L. (2013). Modeling plant species distributions under future climates: How fine scale do climate projections need to be? *Global Change Biology*, *19*(2), 473–483. https://doi.org/10.1111/gcb.12051

Garcia, R. A., Cabeza, M., Rahbek, C., & Araújo, M. B. (2014). Multiple dimensions of climate change and their implications for biodiversity. *Science (New York, N.Y.)*, *344*(6183), 1247579. https://doi.org/10.1126/science.1247579

Geiger, R. (1961). berarbeitete Neuausgabe von Geiger, R: Köppen-Geiger/Klima der Erde. *Wandkarte (wall map)*, *1*, 16.

Gleckler, P. J., Taylor, K. E., & Doutriaux, C. (2008). Performance metrics for climate models. *Journal of Geophysical Research*, *113*(D6), 1147. https://doi.org/10.1029/2007JD008972

Grieser, J., Gommes, R., Cofield, S., & Bernardi, M. (2006). New gridded maps of Koeppen's climate classification.

Hanf, F., Körper, J., Spangehl, T., & Cubasch, U. (2012). Shifts of climate zones in multi-model climate change experiments using the Köppen climate classification. *Meteorologische Zeitschrift*, *21*(2), 111–123. https://doi.org/10.1127/0941-2948/2012/0344

https://doi.org/10.5194/essd-2021-53
Preprint. Discussion started: 24 March 2021

Hansen, M. C., Potapov, P. V., Moore, R., Hancher, M., Turubanova, S. A., Tyukavina, A., . . . Townshend, J. R. G. (2013). High-resolution global maps of 21st-century forest cover change. *Science (New York, N.Y.)*, *342*(6160), 850–853. https://doi.org/10.1126/science.1244693

Hartmann, D. L., A.M.G. Klein Tank, M. Rusticucci, L.V. Alexander, S. Brönnimann, Y. Charabi, . . . P.M. Zhai (2013). *Observations: Atmosphere and Surface*. In: Climate Change 2013: The Physical Science Basis. Contribution of Working Group I to the Fifth Assessment Report of the Intergovernmental Panel on Climate Change [Stocker, T.F., D. Qin, G.-K. Plattner, M. Tignor, S.K. Allen, J. Boschung, A. Nauels, Y. Xia, V. Bex and P.M. Midgley (eds.)]. Cambridge, United Kingdom and New York, NY, USA: Cambridge University Press.

Hay, L. E., Wilby, R. L., & Leavesley, G. H. (2000). A comparison of delta change and downscaled GCM scenarios for three mountainous basins in the united states. *JAWRA Journal of the American Water Resources Association*, *36*(2), 387–397. https://doi.org/10.1111/j.1752-1688.2000.tb04276.x

Hijmans, R. J., Cameron, S. E., Parra, J. L., Jones, P. G., & Jarvis, A. (2005). Very high resolution interpolated climate surfaces for global land areas. *International Journal of Climatology*, *25*(15), 1965–1978. https://doi.org/10.1002/joc.1276

Ho, C. K., Stephenson, D. B., Collins, M., Ferro, C. A. T., & Brown, S. J. (2012). Calibration strategies: A source of additional uncertainty in climate change projections. *Bulletin of the American Meteorological Society*, *93*(1), 21–26. https://doi.org/10.1175/2011BAMS3110.1

Holdridge, L. R. (1947). Determination of world plant formations from simple climatic data. *Science (New York, N.Y.)*, *105*(2727), 367–368. https://doi.org/10.1126/science.105.2727.367

Jones, S. B. (1932). Classifications of North American climates: A review. *Economic Geography*, *8*(2), 205–208. https://doi.org/10.2307/140250

Karger, D. N., Conrad, O., Böhner, J., Kawohl, T., Kreft, H., Soria-Auza, R. W., . . . Kessler, M. (2017). Climatologies at high resolution for the earth's land surface areas. *Scientific Data*, *4*, 170122. https://doi.org/10.1038/sdata.2017.122

Köppen, W. (1900). Versuch einer Klassifikation der Klimate, vorzugsweise nach ihren Beziehungen zur Pflanzenwelt. *Geographische Zeitschrift*, *6*(11), 593–611.

Köppen, W. (1884). Die Wärmezonen der Erde, nach der Dauer der heissen, gemässigten und kalten Zeit und nach der Wirkung der Wärme auf die organische Welt betrachtet. *Meteorologische Zeitschrift*, *1*(21), 5–226.

Köppen, W. P. (1931). Grundriss der klimakunde.

Köppen, W. P. (1936). *Das geographische System der Klimate: Mit 14 Textfiguren*: Borntraeger.

Kottek, M., Grieser, J., Beck, C., Rudolf, B., & Rubel, F. (2006). World map of the Köppen-Geiger climate classification updated. *Meteorologische Zeitschrift*, *15*(3), 259–263. https://doi.org/10.1127/0941-2948/2006/0130

https://doi.org/10.5194/essd-2021-53
Preprint. Discussion started: 24 March 2021

Kriticos, D. J., Webber, B. L., Leriche, A., Ota, N., Macadam, I., Bathols, J., & Scott, J. K. (2012). CliMond: Global high-resolution historical and future scenario climate surfaces for bioclimatic modelling. *Methods in Ecology and Evolution*, *3*(1), 53–64. https://doi.org/10.1111/j.2041-210X.2011.00134.x

Leemans, R., Cramer, W., & van Minnen, J. G. (1996). Prediction of global biome distribution using bioclimatic equilibrium models. *SCOPE-SCIENTIFIC COMMITTEE ON PROBLEMS OF THE ENVIRONMENT INTERNATIONAL COUNCIL OF SCIENTIFIC UNIONS*, *56*, 413–440.

Mahlstein, I., Daniel, J. S., & Solomon, S. (2013). Pace of shifts in climate regions increases with global temperature. *Nature Climate Change*, *3*(8), 739–743. https://doi.org/10.1038/nclimate1876

Manabe, S., & Holloway, J. L. (1975). The seasonal variation of the hydrologic cycle as simulated by a global model of the atmosphere. *Journal of Geophysical Research*, *80*(12), 1617–1649. https://doi.org/10.1029/JC080i012p01617

Menne, M. J., Durre, I., Vose, R. S., Gleason, B. E., & Houston, T. G. (2012). An overview of the global historical climatology network-daily database. Advance online publication. https://doi.org/10.1175/jtech-d-11-00103.1

National Climatic Data Center, NESDIS, NOAA, & U.S. Department of Commerce (2015). Global Surface Summary of the Day - GSOD. Retrieved from https://data.nodc.noaa.gov/cgi-bin/iso?id=gov.noaa.ncdc:C00516#

Navarro-Racines, C., Tarapues, J., Thornton, P., Jarvis, A., & Ramirez-Villegas, J. (2020). High-resolution and bias-corrected CMIP5 projections for climate change impact assessments. *Scientific Data*, *7*(1), 7. https://doi.org/10.1038/s41597-019-0343-8

Netzel, P., & Stepinski, T. (2016). On using a clustering approach for global climate classification. *Journal of Climate*, *29*(9), 3387–3401. https://doi.org/10.1175/JCLI-D-15-0640.1

New, M., Hulme, M., & Jones, P. (2000). Representing twentieth-century space–time climate variability. Part II: Development of 1901–96 monthly grids of terrestrial surface climate. *Journal of Climate*, *13*(13), 2217–2238. https://doi.org/10.1175/1520-0442(2000)013<2217:RTCSTC>2.0.CO;2

Ordonez, A., & Williams, J. W. (2013). Projected climate reshuffling based on multivariate climate-availability, climate-analog, and climate-velocity analyses: Implications for community disaggregation. *Climatic Change*, *119*(3-4), 659–675. https://doi.org/10.1007/s10584-013-0752-1

Peel, M. C., Finlayson, B. L., & McMahon, T. A. (2007). Updated world map of the Köppen-Geiger climate classification. *Hydrology and Earth System Sciences Discussions*, *4*(2), 439–473. https://doi.org/10.5194/hessd-4-439-2007

Peel, M. C., McMahon, T. A., Finlayson, B. L., & Watson, F. G.R. (2001). Identification and explanation of continental differences in the variability of annual runoff. *Journal of Hydrology*, *250*(1-4), 224–240. https://doi.org/10.1016/S0022-1694(01)00438-3

Pinsky, M. L., Worm, B., Fogarty, M. J., Sarmiento, J. L., & Levin, S. A. (2013). Marine taxa track local climate velocities. *Science (New York, N.Y.)*, *341*(6151), 1239–1242. https://doi.org/10.1126/science.1239352

https://doi.org/10.5194/essd-2021-53
Preprint. Discussion started: 24 March 2021

Poulter, B., Ciais, P., Hodson, E., Lischke, H., Maignan, F., Plummer, S., & Zimmermann, N. E. (2011). Plant functional type mapping for earth system models. *Geoscientific Model Development*, *4*(4), 993–1010. https://doi.org/10.5194/gmd-4-993-2011

Roderfeld, H., Blyth, E., Dankers, R., Huse, G., Slagstad, D., Ellingsen, I., . . . Lange, M. A. (2008). Potential impact of climate change on ecosystems of the Barents Sea Region. *Climatic Change*, *87*(1-2), 283–303. https://doi.org/10.1007/s10584-007-9350-4

Rohli, R. V., Andrew, J. T., Reynolds, S. J., Shaw, C., & Vázquez, J. R. (2015). Globally extended Köppen–Geiger climate classification and temporal shifts in terrestrial climatic types. *Physical Geography*, *36*(2), 142–157. https://doi.org/10.1080/02723646.2015.1016382

Rohli, R. V., Joyner, T. A., Reynolds, S. J., & Ballinger, T. J. (2015). Overlap of global Köppen–Geiger climates, biomes, and soil orders. *Physical Geography*, *36*(2), 158–175. https://doi.org/10.1080/02723646.2015.1016384

Rubel, F., Brugger, K., Haslinger, K., & Auer, I. (2017). The climate of the European Alps: Shift of very high resolution Köppen-Geiger climate zones 1800–2100. *Meteorologische Zeitschrift*, *26*(2), 115–125. https://doi.org/10.1127/metz/2016/0816

Rubel, F., & Kottek, M. (2010). Observed and projected climate shifts 1901-2100 depicted by world maps of the Köppen-Geiger climate classification. *Meteorologische Zeitschrift*, *19*(2), 135–141. https://doi.org/10.1127/0941-2948/2010/0430

Rubel, F., & Kottek, M. (2011). Comments on: "The thermal zones of the Earth" by Wladimir Köppen (1884). *Meteorologische Zeitschrift*, *20*(3), 361–365. https://doi.org/10.1127/0941-2948/2011/0285

Russell, R. J. (1931). *Dry climates of the United States: I. Climatic map* (Vol. 5): University of California press.

Sanderson, M. (1999). The Classification of Climates from Pythagoras to Koeppen. *Bulletin of the American Meteorological Society*, *80*(4), 669–673. https://doi.org/10.1175/1520-0477(1999)080<0669:TCOCFP>2.0.CO;2

Schempp, W., Zeller, K., & Duchon, J. (Eds.) (1977). *Splines minimizing rotation-invariant semi-norms in Sobolev spaces: Constructive Theory of Functions of Several Variables*: Springer Berlin Heidelberg.

Sun, Q., Miao, C., Duan, Q., Ashouri, H., Sorooshian, S., & Hsu, K.-L. (2018). A review of global precipitation data sets: Data sources, estimation, and intercomparisons. *Reviews of Geophysics*, *56*(1), 79–107. https://doi.org/10.1002/2017RG000574

Tapiador, F. J., Moreno, R., & Navarro, A. (2019). Consensus in climate classifications for present climate and global warming scenarios. *Atmospheric Research*, *216*, 26–36. https://doi.org/10.1016/j.atmosres.2018.09.017

Tarkan, A. S., & Vilizzi, L. (2015). Patterns, latitudinal clines and countergradient variation in the growth of roach Rutilus rutilus (Cyprinidae) in its Eurasian area of distribution. *Reviews in Fish Biology and Fisheries*, *25*(4), 587–602. https://doi.org/10.1007/s11160-015-9398-6

https://doi.org/10.5194/essd-2021-53
Preprint. Discussion started: 24 March 2021

Taylor, K. E., Stouffer, R. J., & Meehl, G. A. (2012). An overview of CMIP5 and the experiment design. *Bulletin of the American Meteorological Society*, *93*(4), 485–498. https://doi.org/10.1175/BAMS-D-11-00094.1

Tererai, F., & Wood, A. R. (2014). On the present and potential distribution of Ageratina adenophora (Asteraceae) in South Africa. *South African Journal of Botany*, *95*, 152–158. https://doi.org/10.1016/j.sajb.2014.09.001

Thornthwaite, C. W. (1931). The climates of North America: According to a new classification. *Geographical Review*, *21*(4), 633. https://doi.org/10.2307/209372

Thuiller, W., Lavorel, S., Araújo, M. B., Sykes, M. T., & Prentice, I. C. (2005). Climate change threats to plant diversity in Europe. *Proceedings of the National Academy of Sciences of the United States of America*, *102*(23), 8245–8250. https://doi.org/10.1073/pnas.0409902102

Walter, S. D., & Elwood, J. M. (1975). A test for seasonality of events with a variable population at risk. *Journal of Epidemiology & Community Health*, *29*(1), 18–21. https://doi.org/10.1136/jech.29.1.18

Wang, M., & Overland, J. E. (2004). Detecting Arctic climate change using Köppen climate classification. *Climatic Change*, *67*(1), 43–62. https://doi.org/10.1007/s10584-004-4786-2

Webber, B. L., Yates, C. J., Le Maitre, D. C., Scott, J. K., Kriticos, D. J., Ota, N., . . . Midgley, G. F. (2011). Modelling horses for novel climate courses: Insights from projecting potential distributions of native and alien Australian acacias with correlative and mechanistic models. *Diversity and Distributions*, *17*(5), 978–1000. https://doi.org/10.1111/j.1472-4642.2011.00811.x

Willmott, C. J., & Matsuura, K. (2001). Terrestrial air temperature and precipitation: monthly and annual time series (1950 - 1999). Retrieved from http://climate.geog.udel.edu/~climate/html_pages/README.ghcn_ts2.html.

Winsberg, E. (2012). Values and uncertainties in the predictions of global climate models. *Kennedy Institute of Ethics Journal*, *22*(2), 111–137. https://doi.org/10.1353/ken.2012.0008

Yoo, J., & Rohli, R. V. (2016). Global distribution of Köppen–Geiger climate types during the Last Glacial Maximum, Mid-Holocene, and present. *Palaeogeography, Palaeoclimatology, Palaeoecology*, *446*, 326–337. https://doi.org/10.1016/j.palaeo.2015.12.010